Analysis of 1,25-dihydroxyvitamin D_3 genomic action reveals calcium regulating and calcium independent effects in mouse intestine and human enteroids

Shanshan Li[1], Jessica De La Cruz[1], Steven Hutchens[2], Somshuvra Mukhopadhyay[2], Zachary K. Criss[3], Rohit Aita[4], Oscar Pellon-Cardenas[4], Joseph Hur[4], Patricia Soteropoulos[1,5], Seema Husain[1,5], Puneet Dhawan[1,5], Lieve Verlinden[6], Geert Carmeliet[6], James C. Fleet[7], Noah F. Shroyer[3], Michael P. Verzi[4] and Sylvia Christakos[1]*

[1]Department of Microbiology, Biochemistry and Molecular Genetics, Rutgers, The State University of New Jersey, New Jersey Medical School, Newark, New Jersey 07103, [2]Division of Pharmacology and Toxicology, College of Pharmacy, Institute for Cellular and Molecular Biology and Institute for Neuroscience, The University of Texas at Austin, Austin, Texas 78712, [3]Integrative Molecular and Biomedical Sciences Graduate Program, Division of Medicine, Baylor College of Medicine, Houston, Texas 77030, [4]Department of Genetics, Rutgers University, New Brunswick, New Jersey 08854, [5]Genomics Center, Rutgers, The State University of New Jersey, New Jersey Medical School, Newark, New Jersey 07103, [6]Laboratory of Clinical and Experimental Endocrinology, Department of Chronic Diseases and Metabolism, Leuven, Belgium, [7]Department of Nutrition Science, Purdue University, West Lafayette, Indiana 47907

*Corresponding author: Dr. Sylvia Christakos

E-mail: christak@njms.rutgers.edu

Running title: $1,25(OH)_2D_3$ gene regulation in mouse and human intestine

Keywords: calcium, manganese, transporters, intestine, vitamin D, human enteroids, mouse, Slc30a10, TRPV6

Abstract

Although vitamin D is critical for the function of the intestine, most studies have focused on the duodenum. We show that transgenic expression of the vitamin D receptor (VDR) only in the distal intestine of VDR null mice (KO/TG mice) results in the normalization of serum calcium and rescue of rickets. Although it had been suggested that calcium transport in the distal intestine involves a paracellular process, we found that the $1,25(OH)_2D_3$ activated genes in the proximal intestine associated with active calcium transport (*Trpv6*, *S100g*, *Atp2b1*) are also induced by $1,25(OH)_2D_3$ in the distal intestine of KO/TG mice. In addition, *Slc30a10*, a manganese efflux transporter, was one of the genes most induced by $1,25(OH)_2D_3$ in both proximal and distal intestine. Both villus and crypt were found to express *Vdr* and VDR target genes. RNA-seq analysis of human enteroids indicated that the effects of $1,25(OH)_2D_3$ observed in mice are conserved in humans. Using *Slc30a10* $^{-/-}$ mice, a loss of cortical bone and a marked decrease in *S100g* and *Trpv6* in the intestine was observed. Our findings suggest an interrelationship between vitamin D and intestinal Mn efflux and indicate the importance of distal intestinal segments to vitamin D action.

Introduction

The essential role of vitamin D is to mediate calcium homeostasis through its regulatory effects on intestine, bone and kidney (1). Vitamin D has also been reported to affect numerous other physiological processes not involved in calcium regulation including immunomodulatory effects and inhibition of cancer progression (1). The skeletal and extraskeletal effects of $1,25(OH)_2D_3$ (the biologically active from of vitamin D; calcitriol) are mediated by the vitamin D receptor (VDR), a nuclear protein which heterodimerizes with the retinoid X receptor (RXR). VDR/RXR interacts with DNA sequences, vitamin D response elements (VDREs) in target genes and leads to activation or repression of transcription. $1,25(OH)_2D_3$ also recruits coregulatory complexes that participate in the regulation of transcription of VDR target genes. VDR-mediated gene transcription is a multi-step process requiring the spatial and sequential combination of transcriptional coactivators and is influenced by the particular subcellular environment in a gene specific manner (2,3).

A principal target tissue of vitamin D action is the intestine (1,4,5). However, little is known about the molecular targets mediating the effects of vitamin D on intestinal biology. The classic role of $1,25(OH)_2D_3$ is regulation of intestinal calcium absorption which is crucial for bone health. When the need for calcium increases, for example during periods of habitual low calcium intake and during growth, vitamin D mediated intestinal calcium absorption occurs predominantly by an active transcellular process. The most pronounced effects of $1,25(OH)_2D_3$ during the active calcium transport process are increased synthesis of the epithelial calcium channel TRPV6 and the intracellular calcium binding protein calbindin-D_{9k} (4,5). In addition to the active transcellular pathway, calcium can also be absorbed via a non-saturable paracellular process (4,5). Whether $1,25(OH)_2D_3$ regulates calcium absorption by modulating genes associated solely with the facilitated diffusion model or whether $1,25(OH)_2D_3$ affects the paracellular process has been a matter of debate (6-9). Most research on calcium absorption has utilized the proximal small intestine and early studies reported that $1,25(OH)_2D_3$ regulated active calcium transport was localized only in the duodenum (9). It had been suggested that calcium

absorption in the distal intestine reflects vitamin D independent passive diffusion (10). However previous studies also noted that $1,25(OH)_2D_3$ and low dietary calcium can regulate active calcium absorption in the distal intestine of rats (11-13). In addition, we recently showed that transgenic expression of VDR only in the distal intestine (distal ileum, cecum and colon) at levels equivalent to wild type (WT) mice results in normal calcium homeostasis and reverses the VDR dependent rickets of the VDR null mice (14). These findings indicate the importance of the distal intestinal segments to vitamin D action.

Although the classical intestinal role of $1,25(OH)_2D_3$ is regulation of calcium absorption, $1,25(OH)_2D_3$ has been reported to have other important effects on the intestine including protection of the integrity of the mucosal barrier, regulation of pathogen invasion, apoptosis, nutrient transport and cellular differentiation (7,15-19). However, the molecular responses to $1,25(OH)_2D_3$ resulting in these effects in proximal vs. distal intestine are poorly understood. In addition, although intestinal epithelial cells at the villi have been identified as targets for $1,25(OH)_2D_3$, little is known about the effect of $1,25(OH)_2D_3$ in crypts and whether $1,25(OH)_2D_3$ responses occur in crypts has been a matter of debate (20-22). Thus, the diversity and complexity of vitamin D signaling in the intestine have not been fully clarified.

In this study in order to further understand the role of vitamin D in the intestine, we examined the expression of VDR targets using transgenic mice with expression of VDR restricted to the distal intestine (KO/TG mice) (14) and compared our findings in these transgenic mice to vitamin D targets in both proximal and distal intestine of vitamin D deficient mice treated with $1,25(OH)_2D_3$. The classic $1,25(OH)_2D_3$ activated genes found in the proximal intestine and associated with active calcium transport (*Trpv6*, *S100g*, *Atp2b1*) were also induced in the distal intestine. In addition, one of the genes most induced by $1,25(OH)_2D_3$ in the proximal and distal intestine was *Slc30a10*, a manganese (Mn) efflux transporter which has recently been found to be critical for protection against neurotoxicity and liver injury which occur in the presence of elevated Mn levels (23). Both villus and crypts were found to express high levels of VDR and result in $1,25(OH)_2D_3$ mediated target gene induction. RNA-seq analysis of human enteroids confirmed the induction of the same genes in mice and humans (*TRPV6*, *SLC30A10*, *ATP2B1* and *CYP24A1*) in both villus and crypts indicating for the first time direct transcriptomic responses to $1,25(OH)_2D_3$ in human enteroids in both crypt and villus-like

compartments. Studies in *Slc30a10*$^{-/-}$ mice showed a loss of cortical bone and a marked decrease in *S100g* and *Trpv6* in the intestine of these mice. Our findings suggest that 1,25$(OH)_2D_3$ may have a role not only to maintain calcium homeostasis but also in the cellular homeostasis of other divalent ions. Our findings emphasize the importance of the distal as well as the proximal intestine in order to understand intestinal effects of 1,25$(OH)_2D_3$ and that the effects of 1,25$(OH)_2D_3$ involve intestinal epithelial cells in both villus and crypt.

Results

RNA-seq Analysis of Transcriptomic Responses to 1,25$(OH)_2D_3$ in the Colon of Mice with Transgenic Expression of VDR Only in the Distal Intestine

Although most studies have focused on calcium absorption in the proximal intestine, our previous study demonstrated that transgenic expression of VDR only in the distal intestine rescued VDR-dependent rickets observed in the VDR KO mouse. To understand mechanisms by which 1,25$(OH)_2D_3$ acts to regulate intestinal biology not only in the proximal but also in the distal intestine, transcriptomic profiling was done to examine the expression of genes induced by 1,25$(OH)_2D_3$ in the distal intestine of KO/TG mice (KO/TG line 1, noted as TG1) which express VDR exclusively in the distal intestine (distal ileum, cecum and colon) (14; **Fig. 1A, B**). We focused on the colon as a possible unappreciated target for regulation of calcium homeostasis. As noted in **Fig. 1C** the classic 1,25$(OH)_2D_3$ activated genes in the proximal intestine were also the genes most markedly induced by 1,25$(OH)_2D_3$ in the colon of the TG mice (*Cyp24a1*, *Trpv6* and *Sl00g*). Induction of *S100g*, *Trpv6* as well as *Atp2b*, genes involved in active calcium transport (1), suggests that active calcium transport in the distal intestine is involved in the normalization of mineral homeostasis in these mice. Genes associated with passive calcium transport, *Cldn2*, *Cldn12* or *Cacna1d* (Cav1.3 gene) and *Trpm7* which have been suggested as channels other than *Trpv6* for regulation of intestinal calcium absorption (6,24,25), were not significantly regulated by 1,25$(OH)_2D_3$ in the colon. In addition to the classic 1,25$(OH)_2D_3$ activated genes, *Slc30a10*, a manganese efflux transporter located in the apical/luminal domain, was also one of the genes most induced by 1,25$(OH)_2D_3$ and was the principal *Slc* transporter gene affected by 1,25$(OH)_2D_3$. Other *Slc* transporters (*Slc30a1* (a Zn transporter) as well as *Slc30a4* and *Slc30a5* (also Zn transporters; not shown), *Slc39a14* (a Mn transporter which mediates Mn reuptake from the basolateral membrane) and *Slc37a2* (a phosphate linked glucose 6 phosphate antiporter) were

not significantly affected by $1,25(OH)_2D_3$. RT-PCR analysis of intestinal tissues from the same transgenic mouse line (KO/TG1) (**Fig.2A**) as well as from a second independent KO/TG line (KO/TG2, noted as TG2) (**Fig. 2B**) validated the RNA-seq analyses indicating that the genes most responsive to $1,25(OH)_2D_3$ in the distal intestine of KO/TG mice include *Cyp24a1*, *Trpv6*, *Sl00g* and *Slc30a10*. Other *Slc* transporters, *Slc30a1* and *Slc37a2* were unaffected by $1,25(OH)_2D_3$ (**Fig. 2**). Due to the expression of VDR only in the distal intestine, the duodenum of KO/TG mice is unresponsive to $1,25(OH)_2D_3$ (**Fig. 2**; duo).

Regulation of Vitamin D Target Genes in the Intestine

In addition to the induction of *Slc30a10* in the distal intestine of transgenic mice, *Slc30a10* was found to be regulated by $1,25(OH)_2D_3$ in different intestinal segments (duodenum, ileum and colon) of vitamin D deficient mice similar to other vitamin D target genes (*Cyp24a1*, *S100g*). *Slc37a2* although not regulated by $1,25(OH)_2D_3$ in the distal intestine, was induced by $1,25(OH)_2D_3$ in the duodenum (**Fig. 3**). In addition, in the duodenum expression of *Slc30a4*, *Slc30a5*, *Slc39a14*, *Trmp7*, *Cldn12* and *Cacna1d*, similar to findings in the colon (**Fig. 1**) was unaffected by $1,25(OH)_2D_3$ treatment of vitamin D deficient mice (n = 4, vehicle vs. $1,25(OH)_2D_3$ treated; $p > 0.5$). *Cldn2*, however was significantly induced by $1,25(OH)_2D_3$ in the duodenum of these mice (3.8 fold; n=4 vehicle vs. $1,25(OH)_2D_3$ treated; $p < 0.05$).

To gain insight into a possible role of the vitamin D in the regulation of Mn transport, further studies were done comparing the regulation of *Slc30a10* in the intestine to the regulation of known vitamin D target genes. As shown in **Fig. 4A**, *Slc30a10* and *Trpv6* showed a similar time course of induction by $1,25(OH)_2D_3$. Gene expression for these transporters was significantly induced in the duodenum at 4h after injection and then decreased to control levels at 24 h after $1,25(OH)_2D_3$ administration. Similar findings were observed for *Slc30a10* and *Trpv6* in colon (data not shown). These findings suggest a rapid response of *Trpv6* and *Slc30a10* to $1,25(OH)_2D_3$ for intestinal calcium or Mn transport.

In addition to regulation by $1,25(OH)_2D_3$, effects of dietary calcium on the expression of these genes was also examined. Four-week-old mice were fed either a high calcium (1%) or low calcium diet (0.02%) diet for 4 weeks. As shown in **Fig. 4B**, under conditions of low dietary calcium (which results in increased circulating $1,25(OH)_2D_3$ levels) (1) an induction in both *Slc30a10* and *Trpv6* is observed in the duodenum. A similar induction of these genes in response

to low dietary calcium was also observed in the colon (not shown). *S100g* was also significantly increased in duodenum and colon in response to low dietary calcium (data not shown). These findings suggest coregulation of these manganese and calcium transporters under conditions of dietary calcium alteration.

In additional studies developmental changes in the expression of *Slc30a10* and *Trpv6* were compared. *Trpv6* was not expressed significantly in the intestine until after birth and was induced at three weeks of age, the time of weaning in mice which coincides with the increase in active intestinal calcium transport (**Fig. 4C**) (26). Unlike *Trpv6*, *Slc30a10* was detected in the fetal intestine. The most marked induction in the expression of *Slc30a10* was observed between the expression in fetal intestine and at one week postpartum. Thus, developmental changes in intestinal *Slc30a10* and *Trpv6* do not coincide, suggesting that different factors modulate the developmental expression of these transporters.

To further understand a possible interrelationship between vitamin D and manganese homeostasis, vitamin D target genes associated with $1,25(OH)_2D_3$ mediated calcium transport were examined in the intestine of the *Slc30a10*$^{-/-}$ mouse which has manganese levels in blood, brain and liver 20-60 fold higher than controls (27). Expression of *Sl00g* and *Trpv6* was markedly decreased in the duodenum of the *Slc30a10*$^{-/-}$ mice (> 10-fold **Fig. 5A**) but not significantly changed in the colon. Also, no change was observed in the duodenum and colon in the expression of *Tjp1* (ZO-1 gene; previous reports suggested regulation by $1,25(OH)_2D_3$ of intestinal tight junction protein ZO-1) (28). In order to determine the specificity for vitamin D regulated calcium transporters in the intestine, *Trpv5* and *S100g* were examined in the kidney of the *Slc30a10*$^{-/-}$ mice. *S100g* and *Trpv5* were unaffected in the kidney **(Fig. 5B)**.

Micro-computed tomography (μCT) analysis of the tibiae was performed to assess trabecular and cortical parameters in control and *Slc30a10*$^{-/-}$ mice. Trabecular bone mass was slightly, although not significantly, reduced in male *Slc30a10*$^{-/-}$ mice versus control mice, whereas no differences in trabecular bone mass were observed in female mice (**Table 1**). However, a strong cortical bone phenotype was observed in both male and female mice. Tibias of *Slc30a10*$^{-/-}$ mice were smaller in diameter than tibias of control mice as evidenced by their reduced cross-sectional tissue area. In addition, cortical thickness as well as cortical porosity were significantly reduced in *Slc30a10*$^{-/-}$ mice at the mid-diaphysis (**Table 1**). Serum calcium levels were unchanged between *Slc30a10*$^{-/-}$ and control mice (12.5 ± 1.3 vs. 12.3 ± 0.4 ng/ml

respectively; n = 5 , $p > 0.5$) Thus, in addition to the reduction in *Trpv6* and *Sl00g*, there is a significant bone phenotype in these mice.

VDR and Vitamin D Target Genes in Mouse Crypts and Villi and in Differentiated and Undifferentiated Human Enteroids

To provide insight into the mechanisms involved in the regulation of vitamin D target genes in the intestine, including the ion transporters, we examined both mouse villi and crypts. Additionally, human enteroid cultures were used to examine both undifferentiated (crypt-like) and differentiated (villus-like) responses to $1,25(OH)_2D_3$ and to determine whether the effects of $1,25(OH)_2D_3$ in the intestine observed in mice are conserved in humans. Although the importance of vitamin D regulated proteins in intestinal villi has been reported, little is known about effects of $1,25(OH)_2D_3$ in crypts and few findings related to human intestinal VDR targets have been reported. Crypts and villi were isolated from mouse duodenum using the EDTA chelation method (**Fig. 6A**). Expression of *Vdr* as well as VDR protein in mouse villus and crypt was equivalent (**Fig. 6B**). Both villus and crypt respond to $1,25(OH)_2D_3$ by inducing expression of *Cyp24a1* (**Fig. 6C**). *Slc30a10* and *Trpv6*, although more pronounced in villi were also expressed in crypts of WT mice (**Fig. 6D**).

RNA-seq analysis of human duodenal enteroids (**Fig. 7A-C**) showed that intestinal vitamin D target genes are conserved in humans. Similar to the findings in mice, expression of *VDR* under basal conditions was equivalent in villus and crypt compartments. The expression of *VDR* was not significantly affected by $1,25(OH)_2D_3$. However, *TRPV6, SLC30a10, CYP24A1* and *ATP2B1* were significantly upregulated upon $1,25(OH)_2D_3$ treatment in both villus and crypt (**Fig. 7C**). *S100G* was significantly induced by $1,25(OH)_2D_3$ only in villus like cultures. A similar regulation of vitamin D targets genes was observed in crypt-like and villus-like human enteroids derived from the colon (data not shown). Gene expression of *Slc* transporters in addition to *SLC30A10* in differentiated and undifferentiated human duodenal enteroids treated with $1,25(OH)_2D_3$ or vehicle is shown in **Table 2**. *SLC30A4* and *SLC30A5* were not significantly affected by $1,25(OH)_2D_3$. *SLC37A2* was induced in villus but not in crypts. The intestinal phosphate transporter, *SLC34A2*, was upregulated by $1,25(OH)_2D_3$ in both villus and crypt. *TRPM7*, a non-*Slc* transporter, was unaffected by $1,25(OH)_2D_3$ treatment. Gene Ontology (GO) analysis was performed to identify biological processes, cellular components and molecular

function terms that are enriched in human duodenal enteroids treated with $1,25(OH)_2D_3$. The enrichment score [-log10 (p value)] of the terms were plotted to indicate the significance of the enrichment of each function. Regulation of epithelial cell differentiation represented a major category for enrichment of genes by $1,25(OH)_2D_3$ in crypts **(Fig. 8)**. Sonic hedgehog (*SHH*), which controls the proliferation of stem cells, was a $1,25(OH)_2D_3$ target gene in this ontology group as well as response to nutrient, cell migration and cell motility, indicating a role for $1,25(OH)_2D_3$ in the function of stem cells. Pathway analysis indicated enrichment of genes by $1,25(OH)_2D_3$ involved ion transport, oxidation reduction, vitamin D 24-hydroxylase activity, steroid metabolic processes, as well as calcium ion binding and microsomes and vesicular fraction were categories shared in both villus and crypt (**Fig. 8**). $1,25(OH)_2D_3$ target gene members of the gene ontology group identifying microsomes and vesicular fraction include CYP3A4 which is involved in vitamin D metabolism and CYP2C19 and CYP2C18 involved in drug metabolism.

Discussion

Vitamin D plays a major role in maintaining the integrity and function of the intestine as well as in the control of calcium homeostasis. However, the mechanisms by which $1,25(OH)_2D_3$ regulates these processes are not fully understood. Our findings indicate the importance of the distal as well as the proximal segments of the intestine to understand the intestinal effects of $1,25(OH)_2D_3$ and that $1,25(OH)_2D_3$ mediated responses involve epithelial cells in the crypts as well as the villus. This study also shows that the effects of $1,25(OH)_2D_3$ on intestine are complex, are conserved in humans for active calcium uptake and include calcium regulating as well as calcium independent effects in both proximal and distal intestine.

Previous investigations reported that $1,25(OH)_2D_3$ mediated active calcium transport was localized only in the duodenum where the most pronounced effects of $1,25(OH)_2D_3$ during the active calcium transport process were induction of calbindin-D9k (*S100g*) and *Trpv6* (4,5,9). Our current findings indicate that the classic $1,25(OH)_2D_3$ activated genes (*S100g* and *Trpv6*) are also the two genes most markedly induced by $1,25(OH)_2D_3$ in the distal intestine (similar to previous findings in the proximal intestine). In addition, our recent study showing for the first

time a similar VDR-dependent calcium absorption efficiency between proximal colon and duodenum in the same mouse further establishes a role for the distal intestine in VDR-mediated intestinal calcium absorption (29). In that study calcitriol glycosides and glucuronides, which target calcium absorption in the distal intestine, were also found to upregulate *Trpv6* and *S100g* (the genes involved in active calcium transport) as well as calcium absorption in the colon. These results which provide direct in vivo evidence for the importance of VDR in the distal intestine, suggest, together with earlier studies (11-14), that active calcium transport is a vitamin D-dependent process in the distal intestine which plays a role in calcium homeostasis. Calcitriol glucuronide treatment may be a potential means to target calcitriol to the distal intestine and thus compensate for the loss of calcium absorption for example by gastric bypass surgery or small bowel resection. In the current investigation, specific genes previously associated with paracellular calcium transport were not significantly changed by $1,25(OH)_2D_3$ in mouse distal intestine. However, Cldn2 was significantly induced by $1,25(OH)_2D_3$ in the duodenum. Although it is possible that $1,25(OH)_2D_3$ may be involved in paracellular as well as active calcium transport, the physiological relevance of the reported regulation of genes by $1,25(OH)_2D_3$ involved in paracellular transport remains to be determined (6,7,18).

As compared to other tissues, the highest levels of VDR are found in the small and large intestine. Studies related to $1,25(OH)_2D_3$ mediated responses have focused on effects in differentiated enterocytes and have supported a role for $1,25(OH)_2D_3$ in intestinal calcium absorption as well as barrier function (4-7). However, the effect of $1,25(OH)_2D_3$ on intestinal stem cells has not been well investigated and has been a matter of debate (20-22). Previous studies using oral treatment, reported that $1,25(OH)_2D_3$ stimulates *Cyp24a1* in intestinal epithelial cells at the villus or tip region and not at the crypts (20). Early microscopic autoradiographic studies however noted that tritium labeled $1,25(OH)_2D_3$ concentrated in both absorptive and crypt epithelial cells in small and large intestine (30,31). Using a highly specific and sensitive VDR antibody (D6) (32), we also noted, similar to the autoradiographic studies, that VDR is present in villus and crypts. Our studies using isolated mouse villus and crypt as well as human enteroids with either a crypt-like phenotype (high proliferation, undifferentiated) or a villus-like phenotype (low proliferation, differentiated) identified $1,25(OH)_2D_3$ induced target genes, including *Cyp24a1*, in both villus and crypts. The importance of vitamin D in the

function of Lgr5+ stem cells which are sensitive to Wnt stimulation and contribute to intestinal homeostatic regeneration, was previously noted by L. Augenlicht's lab (22). They showed that inactivation of the VDR in mouse Lgr5+ intestinal crypt base columnar cells compromised stem cell functions of the Lgr5+ cells (22). Studies in human colon crypt organoids have also provided evidence that VDR is expressed in intestinal stem cells and has a regulatory role as $1,25(OH)_2D_3$ was found to induce stemness-related genes and to inhibit genes involved in cell proliferation (33). We are now only beginning to understand the regulatory role of vitamin D in intestinal stem cells (22,33,34). It is of interest that both in our *in vivo* studies in mice as well as in our studies using human enteroids, $1,25(OH)_2D_3$ was found to regulate classic target genes in both villus and crypt. These findings suggest, similar to early studies showing the time dependency of $1,25(OH)_2D_3$ action in enterocytes during their differentiation (35), that $1,25(OH)_2D_3$ action in the intestine involves not only calcium absorption but also cellular differentiation and intestinal homeostasis. Although there have been many studies related to the intestinal effects of vitamin D in animals, our findings are one of the few studies examining human vitamin D target genes. Previous studies have been done using human intestinal cell lines derived from colon (19,36-38) as well as human biopsies and duodenal explants (39,40). The limitation of the studies in explants is the inability of the cells to renew as well as cell death in the explants. The enteroid culture system from human tissue allows for growth and maintenance over time and provides an important *in vitro* model to examine both stem and non-stem cell responses to $1,25(OH)_2D_3$. These epithelial cultures of the intestinal tract will provide technology enabling the verification of findings observed in animals and the identification of key components involved in $1,25(OH)_2D_3$ action in human intestinal biology.

In addition to *Cyp24a1*, *Trpv6* and *S100g*, *Slc30a10*, a manganese efflux transporter is also a $1,25(OH)_2D_3$ target gene in both proximal and distal intestine. Slc30a10 is localized in the apical/luminal domain of the intestine, in liver and brain (41). Although initially thought to act as a Zn efflux transporter, recent studies have identified SLC30A10 as a mediator of Mn efflux which lowers cellular Mn levels and protects against Mn toxicity (23,27,42,43). In clinical studies, patients carrying homozygous mutations in *SLC30A10* show enhanced Mn levels, neurotoxicity and liver injury (43,44). It is of interest that Mn levels in the brain are minimally elevated in liver specific Slc30a10 KO mice (41,45). However endoderm specific KO mice

(lacking *Slc30a10* in liver and the gastrointestinal tract) were found to have markedly elevated Mn levels in the brain, indicating a critical role for the digestive system in the regulation of brain manganese (41,45). Our results suggest that $1,25(OH)_2D_3$, by inducing *Slc30a10* in the intestine, may increase Mn excretion and thus may have therapeutic benefit without direct effects on the brain. Preliminary data comparing mice injected with $MnCl_2$ (15 µg/g bw) alone or $MnCl_2$ + $1,25(OH)_2D_3$ (1ng/g bw) 3 times per week for 3 week showed that $1,25(OH)_2D_3$ treatment results in decreased levels of blood Mn (control 30 ± 2.3; Mn, 403 ± 91; Mn ± $1,25(OH)_2D_3$, 288 ± 3.3 ng Mn/ml; S. Mukhopadhyay and S. Christakos, preliminary results). Further studies will be needed to determine effects of $1,25(OH)_2D_3$ on neurotoxicity, on levels of Mn in different tissues as well as effects of vitamin D deficiency, dietary calcium and high dose dietary vitamin D on Mn toxicity. Although elevated levels of Mn are neurotoxic, Mn is an essential element which plays a role in many cellular processes (46). With regard to bone homeostasis, it has been reported that the skeleton is positively influenced by Mn and that deficiency in Mn affects bone mass. Studies in rats have shown that Mn supplementation inhibits ovariectomy induced bone loss (47). In addition, plasma levels of Mn were reported to be significantly decreased in groups of osteoporotic patients (48). More recent studies have noted that local manganese chloride treatment accelerates fracture healing in a rat model (49). However, excess of Mn can adversely affect bone quality. In our study using the Slc30a10 global KO mouse, which exhibits marked elevations in blood Mn, significant cortical bone abnormalities were noted. These findings further indicate the importance of maintaining Mn levels at an optimal range and not exceeding the levels required to accomplish essential functions. The mechanisms involved in the adverse effects on bone observed in the Slc30a10 KO mouse are not known. Whether the reduced thyroxine production observed in the Slc30a10 KO mouse plays a role in the bone phenotype remains to be determined (50). The precise mechanism whereby Mn affects thyroxine biosynthesis is not known. It is of interest that a patient with a loss of function of *SLC30A10* mutation was also identified with hypothyroidism (51).

Due to the necessity of maintaining Mn levels in a narrow range in order to prevent toxicity, understanding the regulation of SLC30A10 is critical. The regulation of *Slc30a10* in the intestine by $1,25(OH)_2D_3$ suggests that $1,25(OH)_2D_3$ not only affects absorption of calcium but may also affect the transport of other divalent cations. The time course of response to

Molecular and Cellular Biology

374 $1,25(OH)_2D_3$ showed that expression of *Trpv6* and *Slc30a10* is significantly elevated 4 h after
375 $1,25(OH)_2D_3$. 24 h after administration of $1,25(OH)_2D_3$ the expression of the genes for both
376 transporters is decreased to levels observed prior to 0 h, consistent with a rapid response of both
377 transporters to $1,25(OH)_2D_3$ as previously noted for *Trpv6* expression (52). The early induction
378 of these transporters would be needed for rapid calcium uptake or Mn efflux. Although putative
379 vitamin D response elements have been noted in the human and mouse gene which encode
380 SLC30A10 (18,19), studies are needed to determine VDR binding sites which are functionally
381 linked to the expression of these genes. The significance of a possible inhibitory effect of
382 unliganded VDR also requires further studies (53,54).

383 To further understand the role of vitamin D in manganese homeostasis, the expression of
384 the classic vitamin D target genes was examined in the intestine of the Slc30a10 KO mouse. In
385 the Slc30a10 KO mouse a marked decrease in the expression of *Trpv6* and *S100g* in the
386 duodenum, a primary route of manganese excretion (55), was consistently observed. These
387 findings suggest that TRPV6, S100G and SLC30A10 may work together in manganese efflux
388 transport. Previous studies using HEK cells transfected with human (h) *TRPV6* showed that
389 TRPV6 is permeable to Mn as well as other heavy metal cations, indicating that TRPV6 is not
390 only involved in calcium transport (56). Since intracellular calcium concentrations have been
391 reported to correlate with the level of expression of TRPV6 (56), our findings of a decrease in
392 *Trpv6* (and *S100g*) in the intestine of mice with Slc30a10 deficiency and defective Mn excretion
393 suggest the possibility of intracellular calcium mediated regulation of intestinal Slc30a10.
394 Kovacs et al observed an inhibition of calcium uptake mediated by TRPV6 in the presence of
395 high concentrations of Mn (56). Therefore, it is also possible that low levels of expression of the
396 genes involved in calcium homeostasis may be due to the high Mn levels in the Slc30a10 KO
397 mice. Although not previously identified *in vivo* in the intestine, an interrelationship between
398 calcium and Mn transport has been noted in other reports including studies in mast cells, in
399 mitochondria and in brain (57-62). It has been suggested that Mn may interfere with brain
400 calcium homeostasis (62). In the mitochondria, Mn transport has been reported to be activated by
401 calcium (58,60). However calcium transport in the mitochondria is inhibited in the presence of
402 Mn (58). In recent studies using HEK cells, it was noted that Slc30a10 extrusion of Mn was
403 calcium-dependent (63). The authors suggested that Slc30a10 uses a calcium gradient for active
404 counter ion exchange (63). Whether Mn efflux transport is regulated in part by calcium in the

intestine (as suggested by our findings) and whether intestinal calcium transport is inhibited in the presence of high blood Mn levels (which are observed in the Slc30a10 KO mouse) remains to be determined. It is possible that the role of the distal intestine, where *Slc30a10* is also induced by $1,25(OH)_2D_3$, may be compensatory when Mn efflux from the proximal intestine is disrupted. The relationship between calcium, the vitamin D endocrine system and Mn efflux in the intestine is an unexplored topic. Since the digestive system has recently been identified as a critical regulator of Mn toxicity (41,45), further studies are needed to provide new insight on the role of calcium and the vitamin D on Mn homeostasis and protection against neurotoxicity.

Findings in our lab as well as prior reports have noted that $1,25(OH)_2D_3$ treatment affects the gene expression of intestinal transporters in addition to *Slc30a10*. Expression of *Slc37a2*, which encodes a phosphate linked glucose 6 phosphate antiporter, was previously shown to be induced by $1,25(OH)_2D_3$ in mouse intestine (18). Although not regulated by $1,25(OH)_2D_3$ in the mouse distal intestine, we found that *SLC37A2* was induced by $1,25(OH)_2D_3$ in human enteroids from duodenum (**Table 2**) and colon (data not shown). Regulation of *SLC37A2* by $1,25(OH)_2D_3$ is not specific to the intestine. *SLC37A2* has also been suggested as a gene target and marker of vitamin D status in hematopoietic cells (64). Although SLC37A2 can transport glucose 6 phosphate (G6P), recent findings suggested that SLC37A2 does not have a role in the regulation of blood glucose (65). Since the functional role of SLC37A2 is not understood at this time, the physiological significance of regulation of gene expression by $1,25(OH)_2D_3$ in both mouse and human intestine remains to be determined. Although we did not find that $1,25(OH)_2D_3$ affected major Zn transporters, previous studies noted regulation of zinc transporters by $1,25(OH)_2D_3$ in mouse intestine (18). Both calcium and zinc are known to play important roles in normal development and bone homeostasis (66-68). Early studies in chicks, however, noted that vitamin D or $1,25(OH)_2D_3$ does not affect zinc absorption in zinc deficient or replete animals (69). Due to the importance of zinc as well as calcium for skeletal integrity, further studies are needed to determine an interrelationship between vitamin D and zinc whether vitamin D has an effect on zinc homeostasis. In addition to regulation of *SLC30A10* as well as *SLC37A2*, *SLC34A2*, the intestinal cotransporter NaPi-IIb was noted to be a gene target induced by $1,25(OH)_2D_3$ in human enteroids derived from duodenum (SLC34A2 is expressed in the proximal intestine in humans and primarily in the ileum in mice). $1,25(OH)_2D_3$ is known to stimulate intestinal phosphate absorption (70) and SLC34A2 has been reported to protect bone when dietary phosphate is

436 restricted (71). However, the role of $1,25(OH)_2D_3$ in the regulation of intestinal SLC34A2 (NaPi-
437 IIb) has been a matter of debate (72-74). Further studies are needed to examine the regulation of
438 this phosphate transporter in human intestine, its physiological significance in bone and
439 phosphate homeostasis in man and whether it has a role in the dysregulation of phosphate
440 observed in chronic kidney disease.

441 In a recent study intestine specific knockout of *Trpm7*, which encodes a channel kinase
442 suggested to control magnesium levels, resulted in decreased serum zinc and calcium levels as
443 well as deceased serum magnesium by post-natal day 5 (mice died by post-natal day 10) (25).
444 The authors suggested that TRPM7 is the common gatekeeper for these ions in the intestine and
445 that TRPM7 and not TRPV6 is the key factor in intestinal calcium absorption. However, these
446 findings were observed in mice prior to the onset of vitamin D receptor mediated active intestinal
447 calcium absorption (which occurs at weaning). In addition, results of our transcriptomic analyses
448 did not indicate regulation of *Trpm7* by $1,25(OH)_2D_3$ in the intestine of mice and *TRPM7*
449 expression was unaffected by $1,25(OH)_2D_3$ treatment in human enteroids. Thus, although
450 TRPM7 is important in early post-natal life, TRPV6 and not TRPM7 is involved in the process
451 of $1,25(OH)_2D_3$ regulated intestinal calcium absorption.

452 In summary, our findings suggest the importance of the distal as well as the proximal
453 intestinal segments in order to understand intestinal effects of vitamin D and that $1,25(OH)_2D_3$
454 effects involve intestinal epithelial cells in both the villus and crypt. In addition, our findings
455 show direct transcriptomic responses to $1,25(OH)_2D_3$ in human enteroids in both villus and crypt
456 and that effects observed in mice are conserved in humans. Since SLC30A10 is the first reported
457 transporter that uses a calcium gradient for active counter ion exchange, our findings suggest that
458 TRPV6, S100G and SLC30A10 work together in Mn transport and that $1,25(OH)_2D_3$ may have a
459 role not only to maintain calcium homeostasis but also in the cellular homeostasis of other
460 divalent ions.

461

462 **Experimental procedures**

463 *Animals* – Studies including the use of wild type (C57BL/6J), KO/TG (mice expressing
464 VDR only in the distal intestine) and *Vdr* knockout (KO) mice were approved by the Rutgers,

New Jersey Medical School Animal Care and Use Committee. Mice were maintained in a virus and parasite-free barrier facility and exposed to a 12h-light, 12h-dark cycle. Food and water were given *ad libitum*.

Transgenic mice expressing VDR only in the distal intestine were generated as previously described (14) using a 9.5 kb fragment from the CDX2 promoter which directs transgene expression specially to the distal intestine (75). The pBSKS-9.5kb CDX2-human(h)VDR poly A transgene was injected into pronuclei of fertilized mouse oocyte at the Rutgers New Jersey Medical School Genome Editing Core Facility. Mice heterozygous for transgene integration and ablation of the endogenous VDR ($TG^{+/-}$, $KO^{+/-}$) were bred to obtain mice with distal intestine specific hVDR expression (TG/KO mice) (Fig. 1A). All TG/KO mice were fed with standard rodent chow diet (Rodent Laboratory Chow 5001; Ralston Purina Co.) and were used at 12- 14 weeks of age. Genotyping was performed by PCR using DNA extracted from tail biopsies and mouse and human specific VDR primers (14). VDR KO mice were obtained from the Jackson Laboratory (originally from M. Demay, Harvard Medical School).

Findings in the TG/KO mouse intestine were compared to results obtained using vitamin D deficient mice. To examine the response to $1,25(OH)_2D_3$ in both TG/KO mice and vitamin D-deficient mice, each animal was administered three intraperitoneal injections of vehicle or $1,25(OH)_2D_3$ (Cayman Chemical Company, Ann Arbor, MI) at a concentration of 1 ng/g body weight (bw) in a 9:1 mix of propylene glycol and ethanol at 48, 24 and 6 hours before termination. The three-dose protocol was used to study short-term and long-term effects of $1,25(OH)_2D_3$ administration.

The vitamin D-deficient mice were generated from C57BL/6J female mice fed a vitamin D deficient diet (-D, 0.47%Ca, 0.3%P; TD89123; Teklad diet from Envigo) for 3-4 weeks before mating, during pregnancy and lactation. Their offspring were provided the same diet starting directly after weaning until the tissues were harvested at 12-14 weeks of age.

Slc30a10 KO (*Slc30a10*$^{-/-}$) mice were generated in the lab of Somshuvra Mukhopadhyay as previously described (27). Tissues from *Slc30a10*$^{-/-}$ mice were obtained at the University of Texas (UT) at Austin under protocols approved by the Institutional Animal Care and Use Committee at UT Austin. Animals were fed regular rodent chow containing ~84 ug Mn/g chow

494 and tissues harvested at 5-6 weeks as knockouts develop severe Mn toxicity beyond 8 weeks of
495 age.

496 In order to compare the regulation of Slc30a10 to the regulation of classic $1,25(OH)_2D_3$
497 target genes a time course of response to $1,25(OH)_2D_3$ as well as the response to high or low
498 calcium diets and developmental changes in the expression of *Slc30a10* were examined. The
499 time course study was conducted using vitamin D-deficient mice injected with a single dose of
500 $1,25(OH)_2D_3$ (ip 10 ng/g bw) and killed at 1,4 or 24h after injection. The dietary study was done
501 using 4-week-old mice fed either a high calcium (1% Ca, TD92309) or low calcium (0.02% Ca
502 TD86162) for 4 weeks. For the developmental study time pregnant, neonatal and adult mice were
503 fed a standard chow diet. Intestine was harvested from 18-day-old fetus and 1-, 3-, and 6-week-
504 old mice (n = 5-6 per group for 1-, 3- and 6-week-old mice; for fetus n = 3 pooled intestinal
505 samples of 3 individual intestines). For the mice studies both male and female mice were studied.
506 No sexual dimorphism was observed in the vitamin D target genes at these ages.

507 To determine whether classical as well as novel responses to $1,25(OH)_2D_3$ occur in both
508 villus and crypt, intestinal epithelial cells were isolated from both crypts and villi. The duodenum
509 from 3-month-old mice was washed in cold phosphate buffered saline (PBS), cut into 1 cm
510 pieces and rotated in 3 mM EDTA in PBS at 4 °C. After vigorous shaking to release the
511 epithelium, crypts were depleted of contaminating villi by passing through a 70 µm cell strainer
512 (BD Falcon, Tewksbury, MA). Villus epithelium was collected from the top of the 70 µm cell
513 strainer (76). To test whether VDR target genes are conserved in humans, human enteroid
514 cultures were used with either a crypt-like phenotype (ie high proliferation, undifferentiated
515 cells) or a villus like phenotype (ie. low proliferation, differentiated cells). Human intestinal
516 tissue specimens were obtained from endoscopy biopsy performed at Baylor College of
517 Medicine (BCM) from adult patients of both sexes (3 females and 3 males; before endoscopy
518 biopsies informed consent was obtained from the patient and the Institutional Review Board at
519 BCM approved this study). Crypts were isolated using the EDTA chelation method described
520 above. For human enteroids crypts were resuspended in Matrigel and plated in a 24 well plate.
521 Enteroids were maintained in complete media with growth factors, CMGF+ with media changes
522 every 2-3 days (77). Enteroids were split every week by passing them through an insulin syringe
523 and replated in Matrigel. For treatment of enteroids with $1,25(OH)_2D_3$ or vehicle, enteroids were

maintained in high Wnt3A (undifferentiated) medium (CMGF+) or differentiation medium (CMGF+ without Wnt3A, nicotinamide, SB202 and R-Spondin) 3 days before treatment, with one media change between (77). Subsequently enteroids were treated with 100 nM $1,25(OH)_2D_3$ (Cayman Chemical Company) or vehicle (ethanol) at equal volumes in media. 24h following treatment enteroids were collected and processed

RNA isolation and expression analysis – Total RNA was isolated from mouse tissues, isolated mouse villus and crypt epithelium and human organoids using RiboZol RNA extraction reagent (Amresco, Solon, OH) or TRIzol reagent (Invitrogen, Carlsbad, CA) according to manufacturer's instructions and subsequently purified with RNeasy Plus Universal Kit (Qiagen, Hilden, Germany) using on column DNAse digestion (Qiagen, Hilden, Germany). RNA concentration was measured with a NanoDrop spectrophotometer ND-1000 (Isogen Life Science, Utrecht, The Netherlands). RNA integrity was assessed using a denaturing agarose gel stained with ethidium bromide (EtBr) or by using an Agilent (Agilent Technologies, Santa Clara, CA) Bioanalyzer nanochip. For quantitative real time PCR (qRT-PCR), 2 µg of total RNA were used to synthesize complementary DNA using Superscript III First Strand synthesis system (Invitrogen, Carlsbad, CA) following the manufacturer's instructions. Relative quantification of target gene expression was performed using Taqman analyses. Taqman Gene Expression Probes (Applied Biosystems, Foster City, CA) used for qRT-PCR are the following: *Cyp24a1* (Mm00487244-m1), *S100g* (Mm00486654-m1), *Slc30a1* (Mm00437377_m1), *Slc30a10* (Mm00437377-m1), *Slc37a2* (Mm00451435_m1), *Trpv5* (Mm01166037_m1), *Trpv6* (Mm00499069-m1) and *Tjp1* (ZO-1 gene; Mm01320638_m1). Reactions were performed in a 7500 Real-Time PCR System (Applied Biosystems, Foster City, CA). The cycle steps were as follow: an initial 3-min incubation at 95 °C, followed by 40 cycles of 95 °C for 10 s, 60 °C for 30 s, and 72 °C for 30 s. Expressions of gene of interest were normalized to *Gapdh* (Mm999999-g1). The $2^{-\Delta\Delta Ct}$ method was used to calculate relative gene expression.

For global assessment of mouse RNA levels, total RNA was subjected to two rounds of poly(A) selection using oligo-d(T)25 magnetic beads (New England Biolabs (NEB), Ipswich, MA) Illumina compatible RNA-seq libraries were constructed using the NEBNext® Ultra™ II RNA Library Prep with Sample Purification Beads (Catalog no. E7775) and NEBNext® Multiplex Oligos for Illumina® (Dual Index Primers Set 1; Catalog No. E7600) according to the

554 manufacturer's instructions. Poly A selection and library quality were assessed using Tapestation
555 2200 (Agilent Technologies, Santa Clara, CA) and libraries were quantified using Qubit 4.0
556 fluorometer (Thermofisher, Waltham, MA). The prepared libraries were sequenced on an
557 Illumina NextSeq 500 instrument. (Illumina, San Diego, CA). CLC Genomics Workbench 11.0.1
558 version (http://www.clcbio.com/products/clc-genomics-workbench/:Qiagen) was used for RNA-
559 seq analysis. De-multiplexed fastq files from RNA-Seq libraries were imported into the CLC
560 software. Bases with low quality were trimmed and reads were aligned to the Mus musculus
561 reference genome build 9 (mm9) using Kallisto. The aligned reads were obtained using the
562 RNA-Seq Analysis tool CLC Genomics Workbench. Kallisto (version 45) was utilized to
563 quantify the transcript abundances of the RNA-Seq samples through pseudoalignment, using
564 single-end reads and an Ensembl mm9 transcriptome build index. The tximport (version 1.14.0)
565 package (78) was run in R (version 3.6.2) to create gene-level count matrices for use with
566 DESeq2 (version 1.26) (79) by importing quantification data obtained from Kallisto. DESeq2
567 was then used to generate transcript levels in each tissue sample. RNA-seq data (GSE 144978)
568 were deposited in the Gene Expression Omnibus of the National Center for Biotechnology.

569 For global assessment of RNA levels from human enteroids samples, RNA-seq data were
570 aligned to the reference human genome (hg38) using Kallsito. Subsequently, differential gene
571 expressions for both mouse and human were assessed using DESeq2 in R and transcript levels
572 were obtained using a false discovery rate of 0.05 and a cut off of 1.5-fold change. RNA-seq data
573 (GSE 159811) were deposited in the Gene Expression Omnibus of the National Center for
574 Biotechnology.

575 For GO term analyses transcript IDS were used with the biomaRt package (version 2.42)
576 (80) along with RDavidWebService package (version 1.24) (81) as well as DAVID 6.8 (82) to
577 identify biological processes, cellular components and molecular functions in which input genes
578 are enriched.

579 *Western blot analysis* – For Western bolt analysis of VDR, total cellular protein was
580 extracted with a lysis buffer containing 50 mM of Tris-HCl (pH 7.5), 150 mM of NaCl, 0.1%
581 sodium dodecyl sulfate, 1.0% NP-40, and protease inhibitors. Protein content was measured
582 using Bradford assay (83) or Reducing Agent and Detergent Compatible Protein Assay (Bio-Rad
583 Laboratories, Inc., Hercules, CA). 50 µg of denatured protein was subjected to sodium dodecyl

sulfate-polyacrylamide gel electrophoresis (4-20% gradient gel; Bio-Rad Laboratories, Inc., Hercules, CA) and transferred onto a polyvinylidene difluoride membrane (Bio-Rad Laboratories, Inc., Hercules, CA) for Western blot analysis using an enhanced chemiluminescent detection system (Denville Scientific, Inc., Holliston, MA). β-actin immunoblotting was used for sample normalization. Anti-VDR (D-6) [research Resource Identified (RRID):AB_628040] and anti-b-actin (RRID:AB_626632) as well as secondary antibodies were obtained from Santa Cruz Biotechnology, Inc. (Dallas, TX).

Bone analysis – µCT analysis of the left tibiae was performed *ex vivo* using a high resolution SkyScan 1172 system (50 kV, 200 µA, 0.5 mm aluminum filter) to examine trabecular and cortical bone parameters (84). Serial tomographs, reconstructed from raw data using the cone-beam reconstruction software (NRecon, v.1.4.4.0; Skyscan), were used to compute trabecular and cortical parameters, respectively from the proximal metaphyseal and mid-diaphyseal area. Analysis was performed according to the guidelines of the American Society for Bone and Mineral Research (85).

Serum analysis – Serum calcium, assayed using a colorimetric assay (Pointe Scientific, Inc. Canton Mi), was determined by Heartland Laboratories, Ames, Iowa.

Statistical analysis – Results are displayed as mean ± standard error (SEM). Data were analyzed using student t-test or ANOVA and additionally with Benjamini and Hochberg in a post-hoc test to consider significant difference between groups ($p < 0.05$).

Acknowledgements

We acknowledge the assistance of M. Aburadi and A. Kyerematen in certain aspects of this investigation.

Author contributions

SL, SC, SM, NFS, MPV and JCF designed the study. SL, JDLC, SH (UT), ZKC, RA, OPC, JH, PD, LV performed experiments. SL, SC, SM, NFS, ZKC, MPV, JCF, GC, LV, PD, PS, SH provided interpretation of results. SL and SC wrote the paper with comments from all authors.

Funding and additional information

This study was supported by NIH grant DK112365 (to S.C., M.P.V., J.C.F and N.F.S.) and NIH grant ESO24812 to S. M. as well as a grant from the FWO:G0A2416N to L.V. and G.C.

Conflict of interest

The authors disclose no conflicts

References

1. Christakos, S., Dhawan, P., Verstuyf, A., Verlinden, L., and Carmeliet, G. (2016) Vitamin D: Metabolism, Molecular Mechanism of Action, and Pleiotropic Effects. *Physiol Rev* **96**, 365-408
2. Pike, J. W., Meyer, M. B., Benkusky, N. A., Lee, S. M., St John, H., Carlson, A., Onal, M., and Shamsuzzaman, S. (2016) Genomic Determinants of Vitamin D-Regulated Gene Expression. *Vitam Horm* **100**, 21-44
3. Pike, J. W., and Christakos, S. (2017) Biology and Mechanisms of Action of the Vitamin D Hormone. *Endocrinol Metab Clin North Am* **46**, 815-843
4. Christakos, S., Lieben, L., Masuyama, R., and Carmeliet, G. (2014) Vitamin D endocrine system and the intestine. *Bonekey Rep* **3**, 496
5. Christakos, S. (2012) Recent advances in our understanding of 1,25-dihydroxyvitamin D(3) regulation of intestinal calcium absorption. *Arch Biochem Biophys* **523**, 73-76
6. Fujita, H., Sugimoto, K., Inatomi, S., Maeda, T., Osanai, M., Uchiyama, Y., Yamamoto, Y., Wada, T., Kojima, T., Yokozaki, H., Yamashita, T., Kato, S., Sawada, N., and Chiba, H. (2008) Tight junction proteins claudin-2 and -12 are critical for vitamin D-dependent Ca2+ absorption between enterocytes. *Mol Biol Cell* **19**, 1912-1921
7. Kutuzova, G. D., and Deluca, H. F. (2004) Gene expression profiles in rat intestine identify pathways for 1,25-dihydroxyvitamin D(3) stimulated calcium absorption and clarify its immunomodulatory properties. *Arch Biochem Biophys* **432**, 152-166
8. Wasserman, R. H., and Fullmer, C. S. (1995) Vitamin D and intestinal calcium transport: facts, speculations and hypotheses. *J Nutr* **125**, 1971S-1979S
9. Pansu, D., Bellaton, C., Roche, C., and Bronner, F. (1983) Duodenal and ileal calcium absorption in the rat and effects of vitamin D. *Am J Physiol* **244**, G695-700
10. Lee, D. B., Hu, M. S., Kayne, L. H., Nakhoul, F., and Jamgotchian, N. (1991) The importance of non-vitamin D-mediated calcium absorption. *Contrib Nephrol* **91**, 14-20
11. Lee, D. B., Walling, M. M., Levine, B. S., Gafter, U., Silis, V., Hodsman, A., and Coburn, J. W. (1981) Intestinal and metabolic effect of 1,25-dihydroxyvitamin D3 in normal adult rat. *Am J Physiol* **240**, G90-96
12. Favus, M. J., Kathpalia, S. C., Coe, F. L., and Mond, A. E. (1980) Effects of diet calcium and 1,25-dihydroxyvitamin D3 on colon calcium active transport. *Am J Physiol* **238**, G75-78
13. Auchere, D., Tardivel, S., Gounelle, J. C., Drueke, T., and Lacour, B. (1998) Role of transcellular pathway in ileal Ca2+ absorption: stimulation by low-Ca2+ diet. *Am J Physiol* **275**, G951-956
14. Dhawan, P., Veldurthy, V., Yehia, G., Hsaio, C., Porta, A., Kim, K. I., Patel, N., Lieben, L., Verlinden, L., Carmeliet, G., and Christakos, S. (2017) Transgenic Expression of the Vitamin D Receptor Restricted to the Ileum, Cecum, and Colon of Vitamin D Receptor Knockout Mice Rescues Vitamin D Receptor-Dependent Rickets. *Endocrinology* **158**, 3792-3804
15. Kong, J., Zhang, Z., Musch, M. W., Ning, G., Sun, J., Hart, J., Bissonnette, M., and Li, Y. C. (2008) Novel role of the vitamin D receptor in maintaining the integrity of the intestinal mucosal barrier. *Am J Physiol Gastrointest Liver Physiol* **294**, G208-216
16. Sun, J. (2010) Vitamin D and mucosal immune function. *Curr Opin Gastroenterol* **26**, 591-595

17. Barbachano, A., Fernandez-Barral, A., Ferrer-Mayorga, G., Costales-Carrera, A., Larriba, M. J., and Munoz, A. (2017) The endocrine vitamin D system in the gut. *Mol Cell Endocrinol* **453**, 79-87
18. Lee, S. M., Riley, E. M., Meyer, M. B., Benkusky, N. A., Plum, L. A., DeLuca, H. F., and Pike, J. W. (2015) 1,25-Dihydroxyvitamin D3 Controls a Cohort of Vitamin D Receptor Target Genes in the Proximal Intestine That Is Enriched for Calcium-regulating Components. *J Biol Chem* **290**, 18199-18215
19. Claro da Silva, T., Hiller, C., Gai, Z., and Kullak-Ublick, G. A. (2016) Vitamin D3 transactivates the zinc and manganese transporter SLC30A10 via the Vitamin D receptor. *J Steroid Biochem Mol Biol* **163**, 77-87
20. Reynolds, C. J., Koszewski, N. J., Horst, R. L., Beitz, D. C., and Goff, J. P. (2019) Localization of the 1,25-dihydroxyvitamin d-mediated response in the intestines of mice. *J Steroid Biochem Mol Biol* **186**, 56-60
21. Colston, K. W., Mackay, A. G., Finlayson, C., Wu, J. C., and Maxwell, J. D. (1994) Localisation of vitamin D receptor in normal human duodenum and in patients with coeliac disease. *Gut* **35**, 1219-1225
22. Peregrina, K., Houston, M., Daroqui, C., Dhima, E., Sellers, R. S., and Augenlicht, L. H. (2015) Vitamin D is a determinant of mouse intestinal Lgr5 stem cell functions. *Carcinogenesis* **36**, 25-31
23. Mukhopadhyay, S. (2018) Familial manganese-induced neurotoxicity due to mutations in SLC30A10 or SLC39A14. *Neurotoxicology* **64**, 278-283
24. Kellett, G. L. (2011) Alternative perspective on intestinal calcium absorption: proposed complementary actions of Ca(v)1.3 and TRPV6. *Nutr Rev* **69**, 347-370
25. Mittermeier, L., Demirkhanyan, L., Stadlbauer, B., Breit, A., Recordati, C., Hilgendorff, A., Matsushita, M., Braun, A., Simmons, D. G., Zakharian, E., Gudermann, T., and Chubanov, V. (2019) TRPM7 is the central gatekeeper of intestinal mineral absorption essential for postnatal survival. *Proc Natl Acad Sci U S A* **116**, 4706-4715
26. Halloran, B. P., and DeLuca, H. F. (1980) Calcium transport in small intestine during early development: role of vitamin D. *Am J Physiol* **239**, G473-479
27. Hutchens, S., Liu, C., Jursa, T., Shawlot, W., Chaffee, B. K., Yin, W., Gore, A. C., Aschner, M., Smith, D. R., and Mukhopadhyay, S. (2017) Deficiency in the manganese efflux transporter SLC30A10 induces severe hypothyroidism in mice. *J Biol Chem* **292**, 9760-9773
28. Zhang, Y. G., Wu, S., and Sun, J. (2013) Vitamin D, Vitamin D Receptor, and Tissue Barriers. *Tissue Barriers* **1**
29. Jiang, H., Horst, R. L., Koszewski, N. J., Goff, J. P., Christakos, S., and Fleet, J. C. (2019) Targeting 1,25(OH)2D-mediated calcium absorption machinery in proximal colon with calcitriol glycosides and glucuronides. *J Steroid Biochem Mol Biol* **198**, 105574
30. Stumpf, W. E., Sar, M., Reid, F. A., Tanaka, Y., and DeLuca, H. F. (1979) Target cells for 1,25-dihydroxyvitamin D3 in intestinal tract, stomach, kidney, skin, pituitary, and parathyroid. *Science* **206**, 1188-1190
31. Stumpf, W. E. (2008) Vitamin D and the digestive system. *Eur J Drug Metab Pharmacokinet* **33**, 85-100
32. Wang, Y., Zhu, J., and DeLuca, H. F. (2012) Where is the vitamin D receptor? *Arch Biochem Biophys* **523**, 123-133
33. Fernandez-Barral, A., Costales-Carrera, A., Buira, S. P., Jung, P., Ferrer-Mayorga, G., Larriba, M. J., Bustamante-Madrid, P., Dominguez, O., Real, F. X., Guerra-Pastrian, L., Lafarga, M., Garcia-Olmo, D., Cantero, R., Del Peso, L., Batlle, E., Rojo, F., Munoz, A., and Barbachano, A. (2020) Vitamin D differentially regulates colon stem cells in patient-derived normal and tumor organoids. *FEBS J* **287**, 53-72

34. Li, W., Peregrina, K., Houston, M., and Augenlicht, L. H. (2019) Vitamin D and the nutritional environment in functions of intestinal stem cells: Implications for tumorigenesis and prevention. *J Steroid Biochem Mol Biol* **198**, 105556
35. Wu, J. C., Smith, M. W., and Lawson, D. E. (1992) Time dependency of 1,25(OH)2D3 induction of calbindin mRNA and calbindin expression in chick enterocytes during their differentiation along the crypt-villus axis. *Differentiation* **51**, 195-200
36. Meyer, M. B., Watanuki, M., Kim, S., Shevde, N. K., and Pike, J. W. (2006) The human transient receptor potential vanilloid type 6 distal promoter contains multiple vitamin D receptor binding sites that mediate activation by 1,25-dihydroxyvitamin D3 in intestinal cells. *Mol Endocrinol* **20**, 1447-1461
37. Wood, R. J., Tchack, L., and Taparia, S. (2001) 1,25-Dihydroxyvitamin D3 increases the expression of the CaT1 epithelial calcium channel in the Caco-2 human intestinal cell line. *BMC Physiol* **1**, 11
38. Fleet, J. C., Eksir, F., Hance, K. W., and Wood, R. J. (2002) Vitamin D-inducible calcium transport and gene expression in three Caco-2 cell lines. *Am J Physiol Gastrointest Liver Physiol* **283**, G618-625
39. Walters, J. R., Balesaria, S., Chavele, K. M., Taylor, V., Berry, J. L., Khair, U., Barley, N. F., van Heel, D. A., Field, J., Hayat, J. O., Bhattacharjee, A., Jeffery, R., and Poulsom, R. (2006) Calcium channel TRPV6 expression in human duodenum: different relationships to the vitamin D system and aging in men and women. *J Bone Miner Res* **21**, 1770-1777
40. Balesaria, S., Sangha, S., and Walters, J. R. (2009) Human duodenum responses to vitamin D metabolites of TRPV6 and other genes involved in calcium absorption. *Am J Physiol Gastrointest Liver Physiol* **297**, G1193-1197
41. Taylor, C. A., Hutchens, S., Liu, C., Jursa, T., Shawlot, W., Aschner, M., Smith, D. R., and Mukhopadhyay, S. (2019) SLC30A10 transporter in the digestive system regulates brain manganese under basal conditions while brain SLC30A10 protects against neurotoxicity. *J Biol Chem* **294**, 1860-1876
42. Leyva-Illades, D., Chen, P., Zogzas, C. E., Hutchens, S., Mercado, J. M., Swaim, C. D., Morrisett, R. A., Bowman, A. B., Aschner, M., and Mukhopadhyay, S. (2014) SLC30A10 is a cell surface-localized manganese efflux transporter, and parkinsonism-causing mutations block its intracellular trafficking and efflux activity. *J Neurosci* **34**, 14079-14095
43. Tuschl, K., Clayton, P. T., Gospe, S. M., Jr., Gulab, S., Ibrahim, S., Singhi, P., Aulakh, R., Ribeiro, R. T., Barsottini, O. G., Zaki, M. S., Del Rosario, M. L., Dyack, S., Price, V., Rideout, A., Gordon, K., Wevers, R. A., Chong, W. K., and Mills, P. B. (2012) Syndrome of hepatic cirrhosis, dystonia, polycythemia, and hypermanganesemia caused by mutations in SLC30A10, a manganese transporter in man. *Am J Hum Genet* **90**, 457-466
44. Quadri, M., Federico, A., Zhao, T., Breedveld, G. J., Battisti, C., Delnooz, C., Severijnen, L. A., Di Toro Mammarella, L., Mignarri, A., Monti, L., Sanna, A., Lu, P., Punzo, F., Cossu, G., Willemsen, R., Rasi, F., Oostra, B. A., van de Warrenburg, B. P., and Bonifati, V. (2012) Mutations in SLC30A10 cause parkinsonism and dystonia with hypermanganesemia, polycythemia, and chronic liver disease. *Am J Hum Genet* **90**, 467-477
45. Mercadante, C. J., Prajapati, M., Conboy, H. L., Dash, M. E., Herrera, C., Pettiglio, M. A., Cintron-Rivera, L., Salesky, M. A., Rao, D. B., and Bartnikas, T. B. (2019) Manganese transporter Slc30a10 controls physiological manganese excretion and toxicity. *J Clin Invest* **129**, 5442-5461
46. Chen, P., Bornhorst, J., and Aschner, M. (2018) Manganese metabolism in humans. *Front Biosci (Landmark Ed)* **23**, 1655-1679
47. Rico, H., Gomez-Raso, N., Revilla, M., Hernandez, E. R., Seco, C., Paez, E., and Crespo, E. (2000) Effects on bone loss of manganese alone or with copper supplement in ovariectomized rats. A morphometric and densitomeric study. *Eur J Obstet Gynecol Reprod Biol* **90**, 97-101

48. Heaney, R. P. (1988) Nutritional factors in causation of osteoporosis. *Ann Chir Gynaecol* **77**, 176-179

49. Hreha, J., Wey, A., Cunningham, C., Krell, E. S., Brietbart, E. A., Paglia, D. N., Montemurro, N. J., Nguyen, D. A., Lee, Y. J., Komlos, D., Lim, E., Benevenia, J., O'Connor, J. P., and Lin, S. S. (2015) Local manganese chloride treatment accelerates fracture healing in a rat model. *J Orthop Res* **33**, 122-130

50. Liu, C., Hutchens, S., Jursa, T., Shawlot, W., Polishchuk, E. V., Polishchuk, R. S., Dray, B. K., Gore, A. C., Aschner, M., Smith, D. R., and Mukhopadhyay, S. (2017) Hypothyroidism induced by loss of the manganese efflux transporter SLC30A10 may be explained by reduced thyroxine production. *J Biol Chem* **292**, 16605-16615

51. Anagianni, S., and Tuschl, K. (2019) Genetic Disorders of Manganese Metabolism. *Curr Neurol Neurosci Rep* **19**, 33

52. Song, Y., Peng, X., Porta, A., Takanaga, H., Peng, J. B., Hediger, M. A., Fleet, J. C., and Christakos, S. (2003) Calcium transporter 1 and epithelial calcium channel messenger ribonucleic acid are differentially regulated by 1,25 dihydroxyvitamin D3 in the intestine and kidney of mice. *Endocrinology* **144**, 3885-3894

53. Huet, T., Laverny, G., Ciesielski, F., Molnar, F., Ramamoorthy, T. G., Belorusova, A. Y., Antony, P., Potier, N., Metzger, D., Moras, D., and Rochel, N. (2015) A vitamin D receptor selectively activated by gemini analogs reveals ligand dependent and independent effects. *Cell Rep* **10**, 516-526

54. Lee, S. M., and Pike, J. W. (2016) The vitamin D receptor functions as a transcription regulator in the absence of 1,25-dihydroxyvitamin D3. *J Steroid Biochem Mol Biol* **164**, 265-270

55. Bertinchamps, A. J., Miller, S. T., and Cotzias, G. C. (1966) Interdependence of routes excreting manganese. *Am J Physiol* **211**, 217-224

56. Kovacs, G., Danko, T., Bergeron, M. J., Balazs, B., Suzuki, Y., Zsembery, A., and Hediger, M. A. (2011) Heavy metal cations permeate the TRPV6 epithelial cation channel. *Cell Calcium* **49**, 43-55

57. Fasolato, C., Hoth, M., Matthews, G., and Penner, R. (1993) Ca2+ and Mn2+ influx through receptor-mediated activation of nonspecific cation channels in mast cells. *Proc Natl Acad Sci U S A* **90**, 3068-3072

58. Gavin, C. E., Gunter, K. K., and Gunter, T. E. (1999) Manganese and calcium transport in mitochondria: implications for manganese toxicity. *Neurotoxicology* **20**, 445-453

59. Kamer, K. J., Sancak, Y., Fomina, Y., Meisel, J. D., Chaudhuri, D., Grabarek, Z., and Mootha, V. K. (2018) MICU1 imparts the mitochondrial uniporter with the ability to discriminate between Ca(2+) and Mn(2+). *Proc Natl Acad Sci U S A* **115**, E7960-E7969

60. Vinogradov, A., and Scarpa, A. (1973) The initial velocities of calcium uptake by rat liver mitochondria. *J Biol Chem* **248**, 5527-5531

61. Ijomone, O. M., Aluko, O. M., Okoh, C. O. A., Martins, A. C., Jr., and Aschner, M. (2019) Role for calcium signaling in manganese neurotoxicity. *J Trace Elem Med Biol* **56**, 146-155

62. Bornhorst, J., Wehe, C. A., Huwel, S., Karst, U., Galla, H. J., and Schwerdtle, T. (2012) Impact of manganese on and transfer across blood-brain and blood-cerebrospinal fluid barrier in vitro. *J Biol Chem* **287**, 17140-17151

63. Levy, M., Elkoshi, N., Barber-Zucker, S., Hoch, E., Zarivach, R., Hershfinkel, M., and Sekler, I. (2019) Zinc transporter 10 (ZnT10)-dependent extrusion of cellular Mn(2+) is driven by an active Ca(2+)-coupled exchange. *J Biol Chem* **294**, 5879-5889

64. Wilfinger, J., Seuter, S., Tuomainen, T. P., Virtanen, J. K., Voutilainen, S., Nurmi, T., de Mello, V. D., Uusitupa, M., and Carlberg, C. (2014) Primary vitamin D receptor target genes as biomarkers for the vitamin D3 status in the hematopoietic system. *J Nutr Biochem* **25**, 875-884

65. Pan, C. J., Chen, S. Y., Jun, H. S., Lin, S. R., Mansfield, B. C., and Chou, J. Y. (2011) SLC37A1 and SLC37A2 are phosphate-linked, glucose-6-phosphate antiporters. *PLoS One* **6**, e23157
66. Cousins, R. J. (2010) Gastrointestinal factors influencing zinc absorption and homeostasis. *Int J Vitam Nutr Res* **80**, 243-248
67. Rossi, L., Migliaccio, S., Corsi, A., Marzia, M., Bianco, P., Teti, A., Gambelli, L., Cianfarani, S., Paoletti, F., and Branca, F. (2001) Reduced growth and skeletal changes in zinc-deficient growing rats are due to impaired growth plate activity and inanition. *J Nutr* **131**, 1142-1146
68. Lieben, L., Carmeliet, G., and Masuyama, R. (2011) Calcemic actions of vitamin D: effects on the intestine, kidney and bone. *Best Pract Res Clin Endocrinol Metab* **25**, 561-572
69. Koo, S. I., Fullmer, C. S., and Wasserman, R. H. (1980) Effect to cholecalciferol and 1,25-Dihydroxycholecalciferol on the intestinal absorption of zinc in the chick. *J Nutr* **110**, 1813-1818
70. Williams, K. B., and DeLuca, H. F. (2007) Characterization of intestinal phosphate absorption using a novel in vivo method. *Am J Physiol Endocrinol Metab* **292**, E1917-1921
71. Knopfel, T., Pastor-Arroyo, E. M., Schnitzbauer, U., Kratschmar, D. V., Odermatt, A., Pellegrini, G., Hernando, N., and Wagner, C. A. (2017) The intestinal phosphate transporter NaPi-IIb (Slc34a2) is required to protect bone during dietary phosphate restriction. *Sci Rep* **7**, 11018
72. Marks, J. (2019) The role of SLC34A2 in intestinal phosphate absorption and phosphate homeostasis. *Pflugers Arch* **471**, 165-173
73. Katai, K., Miyamoto, K., Kishida, S., Segawa, H., Nii, T., Tanaka, H., Tani, Y., Arai, H., Tatsumi, S., Morita, K., Taketani, Y., and Takeda, E. (1999) Regulation of intestinal Na+-dependent phosphate co-transporters by a low-phosphate diet and 1,25-dihydroxyvitamin D3. *Biochem J* **343 Pt 3**, 705-712
74. Capuano, P., Radanovic, T., Wagner, C. A., Bacic, D., Kato, S., Uchiyama, Y., St-Arnoud, R., Murer, H., and Biber, J. (2005) Intestinal and renal adaptation to a low-Pi diet of type II NaPi cotransporters in vitamin D receptor- and 1alphaOHase-deficient mice. *Am J Physiol Cell Physiol* **288**, C429-434
75. Hinoi, T., Akyol, A., Theisen, B. K., Ferguson, D. O., Greenson, J. K., Williams, B. O., Cho, K. R., and Fearon, E. R. (2007) Mouse model of colonic adenoma-carcinoma progression based on somatic Apc inactivation. *Cancer Res* **67**, 9721-9730
76. Chen, L., Vasoya, R. P., Toke, N. H., Parthasarathy, A., Luo, S., Chiles, E., Flores, J., Gao, N., Bonder, E. M., Su, X., and Verzi, M. P. (2019) HNF4 Regulates Fatty Acid Oxidation and is Required for Renewal of Intestinal Stem Cells in Mice. *Gastroenterology*
77. Mahe, M. M., Sundaram, N., Watson, C. L., Shroyer, N. F., and Helmrath, M. A. (2015) Establishment of human epithelial enteroids and colonoids from whole tissue and biopsy. *J Vis Exp*
78. Soneson, C., Love, M. I., and Robinson, M. D. (2015) Differential analyses for RNA-seq: transcript-level estimates improve gene-level inferences. *F1000Res* **4**, 1521
79. Love, M. I., Huber, W., and Anders, S. (2014) Moderated estimation of fold change and dispersion for RNA-seq data with DESeq2. *Genome Biol* **15**, 550
80. Durinck, S., Spellman, P. T., Birney, E., and Huber, W. (2009) Mapping identifiers for the integration of genomic datasets with the R/Bioconductor package biomaRt. *Nat Protoc* **4**, 1184-1191
81. Fresno, C., and Fernandez, E. A. (2013) RDAVIDWebService: a versatile R interface to DAVID. *Bioinformatics* **29**, 2810-2811
82. Huang da, W., Sherman, B. T., and Lempicki, R. A. (2009) Systematic and integrative analysis of large gene lists using DAVID bioinformatics resources. *Nat Protoc* **4**, 44-57
83. Bradford, M. M. (1976) A rapid and sensitive method for the quantitation of microgram quantities of protein utilizing the principle of protein-dye binding. *Anal Biochem* **72**, 248-254

84. Lieben, L., Benn, B. S., Ajibade, D., Stockmans, I., Moermans, K., Hediger, M. A., Peng, J. B., Christakos, S., Bouillon, R., and Carmeliet, G. (2010) Trpv6 mediates intestinal calcium absorption during calcium restriction and contributes to bone homeostasis. *Bone* **47**, 301-308

85. Bouxsein, M. L., Boyd, S. K., Christiansen, B. A., Guldberg, R. E., Jepsen, K. J., and Muller, R. (2010) Guidelines for assessment of bone microstructure in rodents using micro-computed tomography. *J Bone Miner Res* **25**, 1468-1486

Footnotes

The abbreviations used are: $1,25(OH)_2D_3$, 1,25-dihydroxyvitamin D3; $25(OH)D_3$, 25-hydroxyvitamin D_3; ANOVA, Analysis of variance; bw, body weight; CYP24A1, 25-hydroxyvitamin D_3 24-Hydroxylase; DNA, deoxyribonucleic acid; EDTA, ethylenediaminetetraacetate; g, gram; HCL, hydrogen chloride; hVDR, human VDR; kb, kilobases; kDa, kilodaltons; KO, knockout; KO/TG, knockout/transgenic; µCT, micro-computed tomography; min, minute(s); Mn, manganese; mRNA, messenger RNA; NaPi-IIb, Sodium-dependent phosphate transport protein 2B; ng, nanogram; PBS, phosphate-buffered saline; RNA-Seq, RNA sequencing; S100g, RT-qPCR, quantitative reverse transcription PCR; S100 calcium binding protein G; SEM, standard error of the mean; Slc30a1, zinc transporter 1; SLC30A10, Solute Carrier Family 30 Member 10; SLC30A4, Solute Carrier Family 30 Member 4; SLC30A5, solute carrier family 30 member 5; SLC34A2, Sodium-dependent phosphate transport protein 2B; SLC37A2, Glucose-6-phosphate exchanger; Tris, tris(hydroxymethyl)aminomethane; TRPV6, Transient receptor potential cation channel subfamily V member 6; VDR, vitamin D receptor; VDRE, vitamin D response element; Zn, zinc

Figure Legends

Figure 1. Gene expression measured by RNA-seq in the colon of KO/TG1 mice treated with $1,25(OH)_2D_3$ (A) KO/TG mice express VDR only in the distal intestine. Expression of hVDR is restricted to the distal intestine of KO/TG mice. Mouse (m) VDR is absent in KO/TG mice. (B) Rescue of VDR dependent rickets in the KO/TG mice (Von Kossa staining; see ref 14). (C) Gene expression in the colon of KO/TG mice treated with $1,25(OH)_2D_3$ (TG1 +D, black bar) compared to VDR KO (open bar). Gene expression, measured by RNA-seq analysis, is shown as the mean of RPKM ± SEM. n = 4 per group * $p < 0.05$, TG1 + D compared to VDR KO.

Figure 2. Response to $1,25(OH)_2D_3$ treatment in KO/TG mouse intestine as measured by RT-qPCR. Gene expression in the duodenum (Duo) and colon (Col) of KO/TG1 mice (TG1) (A) or KO/TG2 mice [mice from a second transgenic line (TG2)] (B) treated with vehicle (black bar) or $1,25(OH)_2D_3$ (1 ng/g bw at 48, 24 and 6 h before termination; TG1+ D or TG2 + D, stripped bar). Results are compared to VDR KO mice (open bar). n = 6 per experimental group. Gene expression was normalized to *Gapdh* and expressed as mean ± SEM (+ $p < 0.05$ compared to vehicle (TG1 or TG2), # $p < 0.05$ $1,25(OH)_2D_3$ treated (TG1 or TG2 +D) compared to VDR KO; * $p < 0.05$ vehicle (TG1 or TG2) compared to VDR KO. The duodenum was included as a control. Note the lack of responsiveness of the duodenum to $1,25(OH)_2D_3$ treatment due to the absence of VDR in the proximal intestine of these transgenic mice. Col, colon; Duo, duodenum; ND, not detected.

Figure 3. Gene expression in intestinal segments in response to repeated administration of $1,25(OH)_2D_3$ to vitamin D deficient mice. 12- to 14-week-old vitamin D-deficient mice were injected with $1,25(OH)_2D_3$ (+D, black bar) or vehicle (open bar) three times over 48 h (at 48, 24 and 6 h prior to termination (ip. 1ng/g bw per injection). Data was normalized to *Gapdh* and expressed as mean ± SEM. n = 6 per experimental group. * Significantly different from vehicle treated group at $p < 0.05$. Duo, duodenum; Ile, ileum; Col, colon; ND, not detected.

Figure 4. Regulation of intestinal $1,25(OH)_2D_3$ target gene expression: time course of induction by $1,25(OH)_2D_3$, effects of dietary calcium and developmental changes. (A) RT-qPCR analysis of *Slc30a10* and *Trpv6* expression in the duodenum at 0, 4 and 24 h after a single injection of $1,25(OH)_2D_3$ (10 ng/g bw) to vitamin D deficient mice. n = 5 per time point. * $p < 0.05$ compared to 0 time point. (B) RT-qPCR analysis of *Slc30a10* and *Trpv6* expression in duodenum of mice fed a low calcium (0.02%) or high calcium (1%) diet for 4 weeks. n = 7 per group. * Significantly different from the mice fed the high calcium diet at $p < 0.05$. (C) Developmental changes in gene expression in mice raised under standard conditions and killed at

18 days gestation and at 1, 3, and 6 weeks of age. Intestine was harvested (for fetus n = 5, pooled intestinal samples of 3 - 4 individual intestines; n = 5 - 6 for 1-, 3-, and 6-week-old mice). Since the small intestine and not individual segments were harvested and analyzed in the fetus, for comparison small intestine was also analyzed at different post-natal stages. Data are expressed as mean ± SEM. Data were normalized using *Gapdh* or *18S rRNA*. # Significantly different from fetus at $p < 0.05$. * Significantly different from 1 week old at $p < 0.05$. Duo, duodenum.

Figure 5. $1,25(OH)_2D_3$ target gene expression in the intestine and kidney of *Slc30a10*$^{-/-}$ and control mice. $1,25(OH)_2D_3$ target genes in the intestine (A) and kidney (B) in *Slc30a10*$^{-/-}$ and control mice. Data are expressed as mean ± SEM and were normalized using *Gapdh*. n = 4 - 6 in each group. * $p < 0.05$ significantly different between two experimental groups. Duo, duodenum; Col, colon.

Figure 6. VDR and $1,25(OH)_2D_3$ target genes in mouse epithelial cells in villi and crypts. (A) Intestinal epithelial cells were isolated from crypts (left panel) and villi (right panel) of 3-month-old mouse duodenum. (B) *Vdr* gene expression (left panel) and VDR protein (Western blot analysis; right panel) in mouse duodenal crypts and villi from 3-month-old WT mice compared to VDR KO mice. For Western blot analysis the relative optical density (OD) obtained using the VDR antibody was divided by the OD obtained after β-actin staining to produce VDR-relative OD. n= 3 - 4 (C and D) RT-qPCR analysis of $1,25(OH)_2D_3$ target genes in mouse duodenal villi and crypts. (C) *Cyp24a1* expression was examined in 3-month-old mice injected ip. with vehicle or $1,25(OH)_2D_3$ (1 ng/g bw; injected at 48, 24, and 6 h prior to euthanasia). * significantly different from WT + vehicle at $p < 0.05$. (D) *Trpv6* and *Slc30a10* gene expression in intestinal epithelial cells from crypts and villi of 3-month-old WT mice. RT-qPCR reactions were normalized to *Gapdh* or *18S rRNA*. n = 3 - 4. ND, not detected.

Figure 7. Gene expression measured by RNA-seq in crypt-like and villus-like human duodenal organoids. (A) Bright field images of crypt-like (undifferentiated) and villus-like (differentiated) duodenal human enteroids. (B) Venn diagram indicating genes significantly upregulated at least 1.5 folds and with FDR < 0.05 upon $1,25(OH)_2D_3$ treatment (100 nM for 24 h) in crypt-like (undifferentiated) and villus-like (differentiated) human enteroids and overlapping genes. (C) Expression counts of *SLC30A10*, *VDR* and classic $1,25(OH)_2D_3$ target genes in control and $1,25(OH)_2D_3$ treated villus and crypt-like human enteroids. Data is from enteroids from 6 patients (3 females and 3 males).

Figure 8. Top GO terms for genes enriched in human duodenal enteroids treated with $1,25(OH)_2D_3$ (A) Crypt only (B) Villus only (C) Crypt and Villus shared.

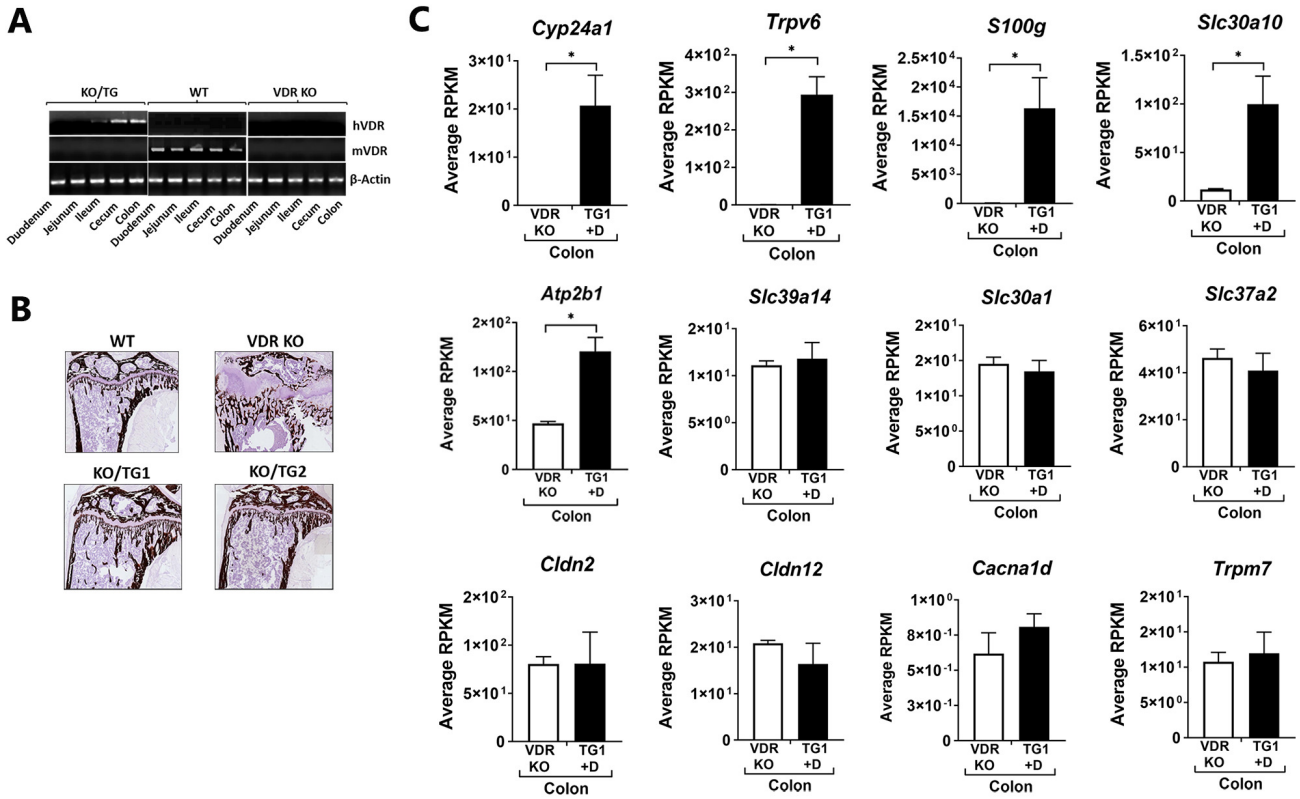

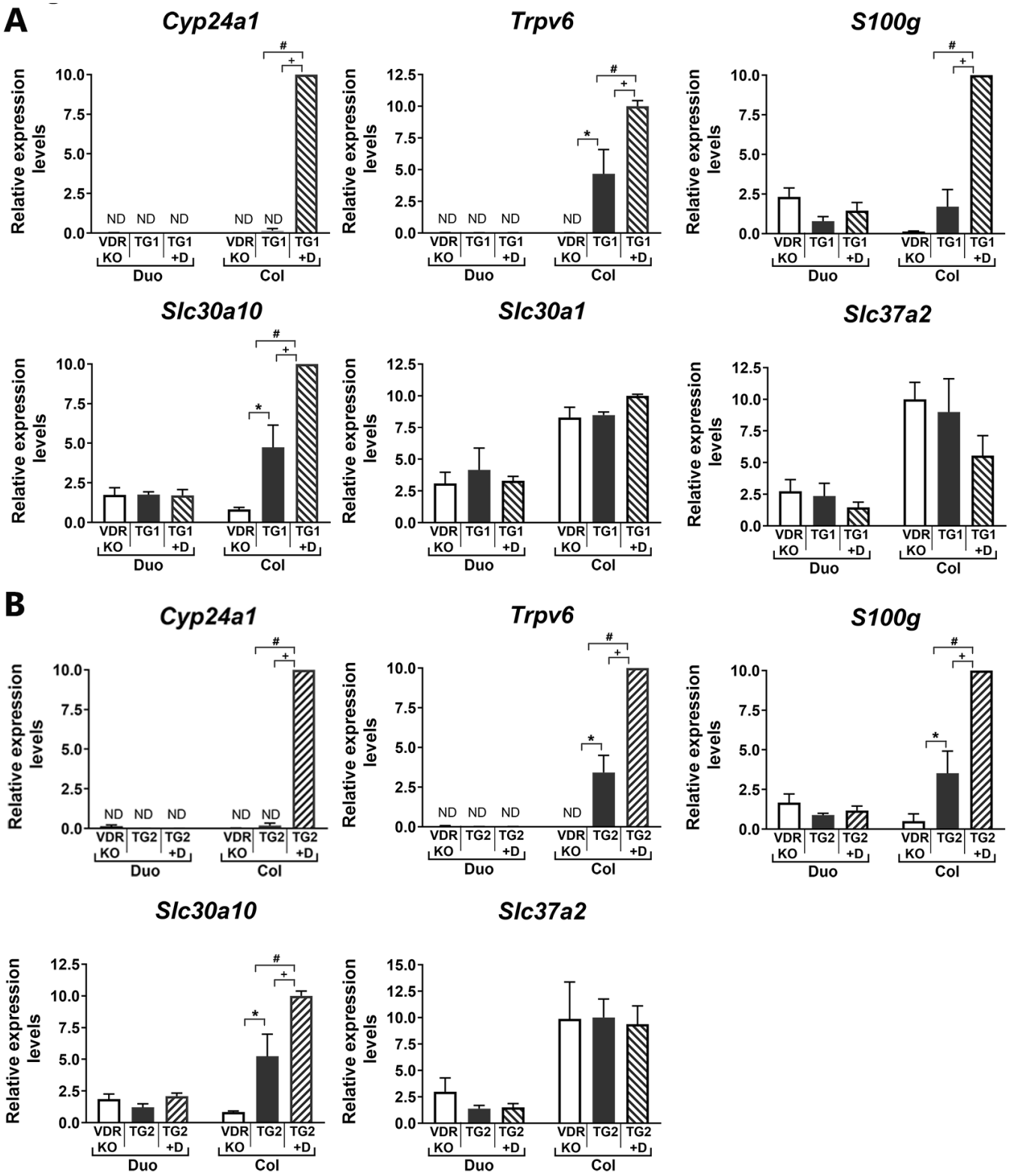

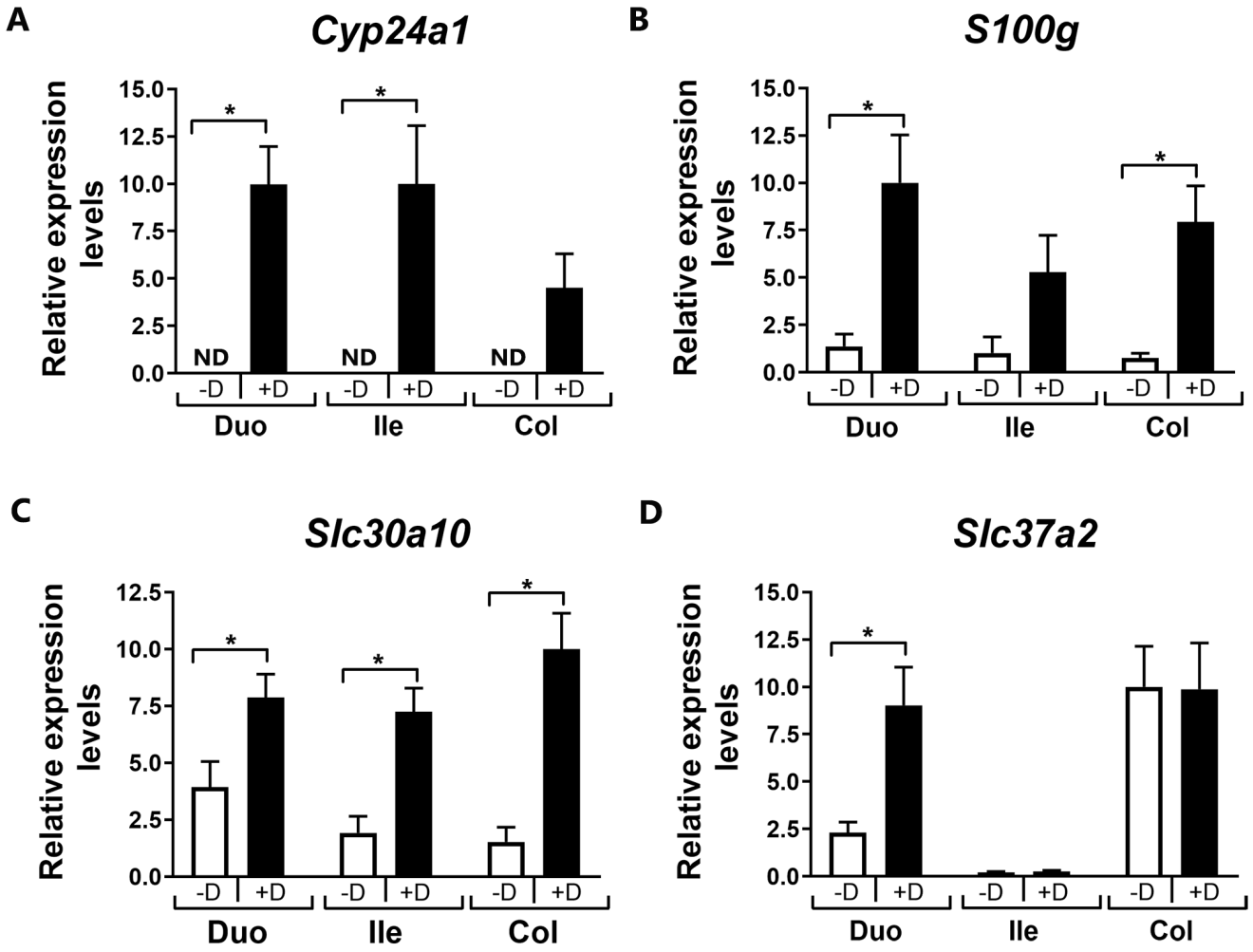

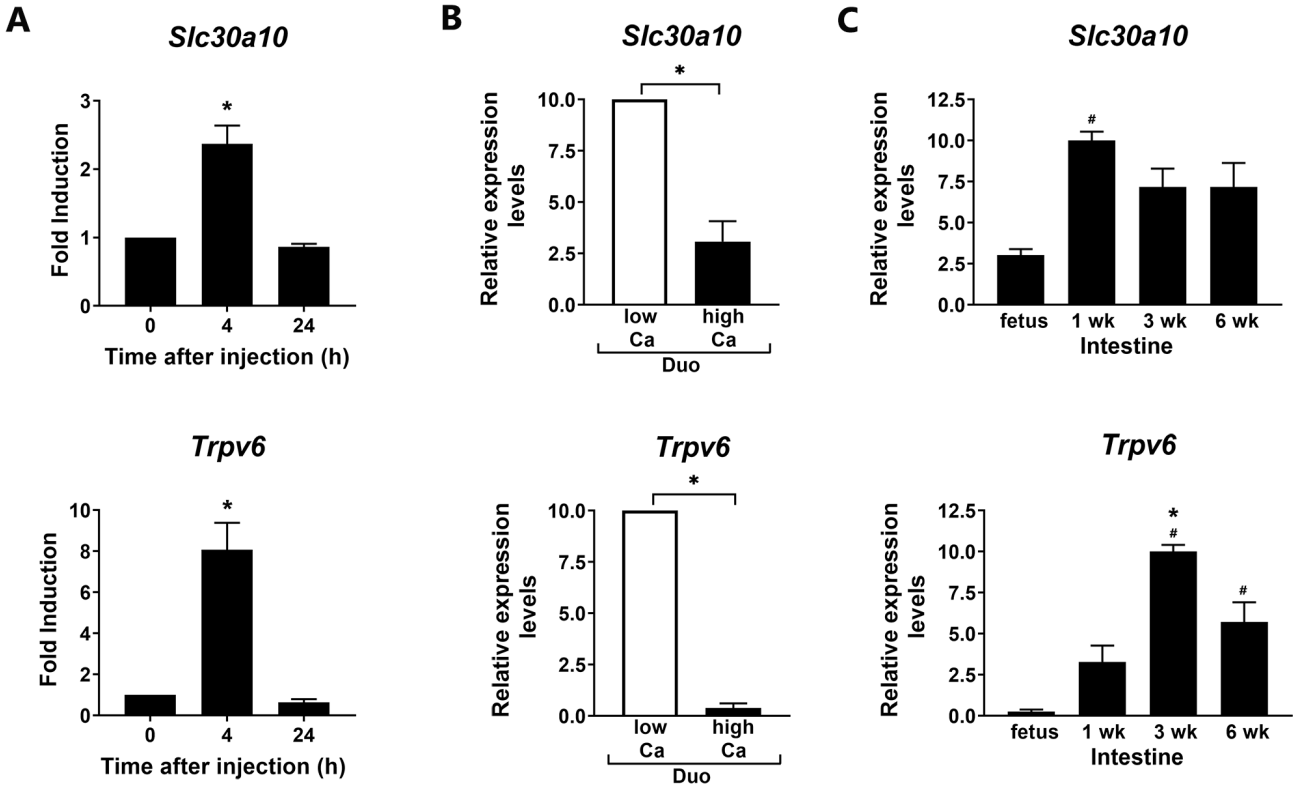

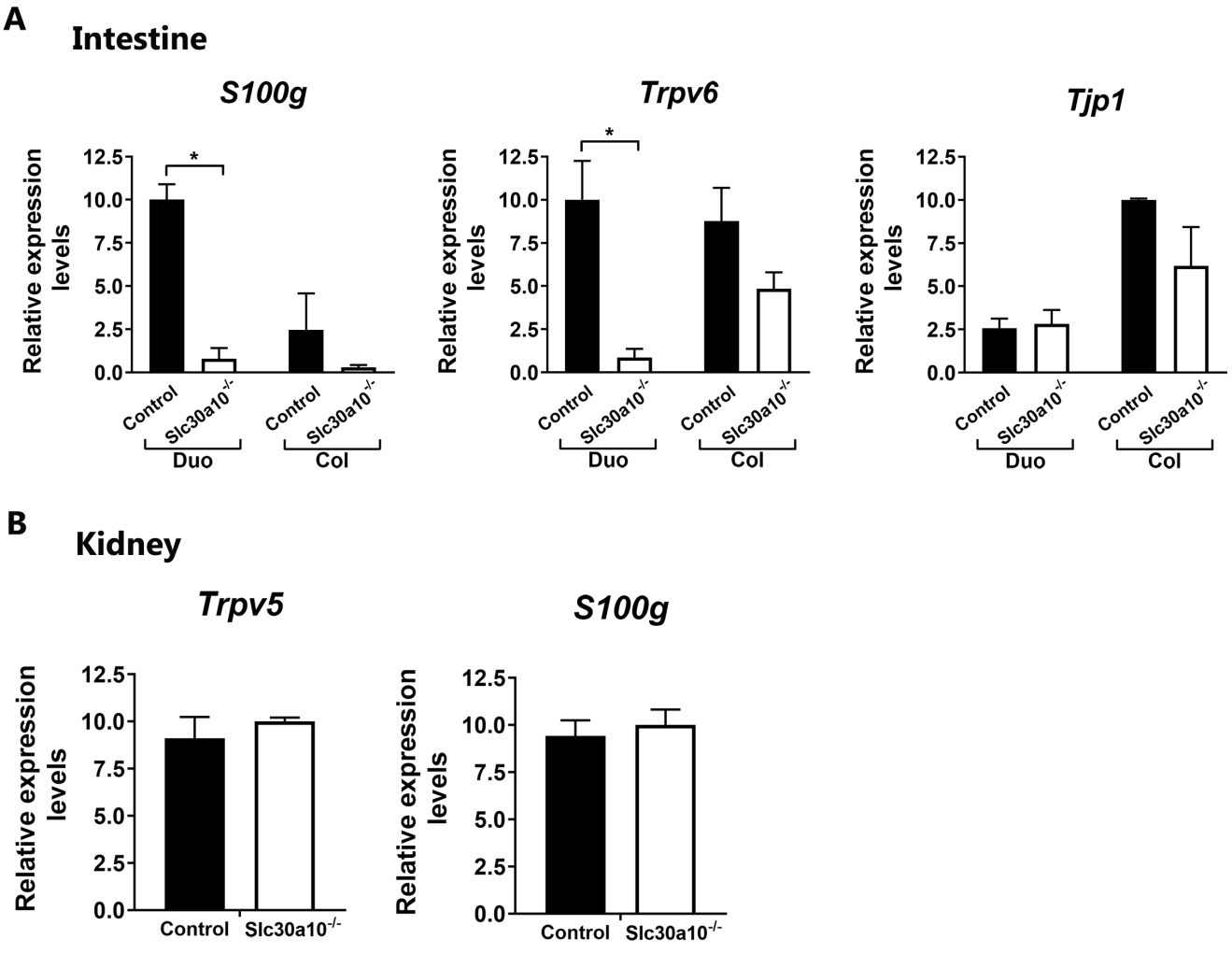

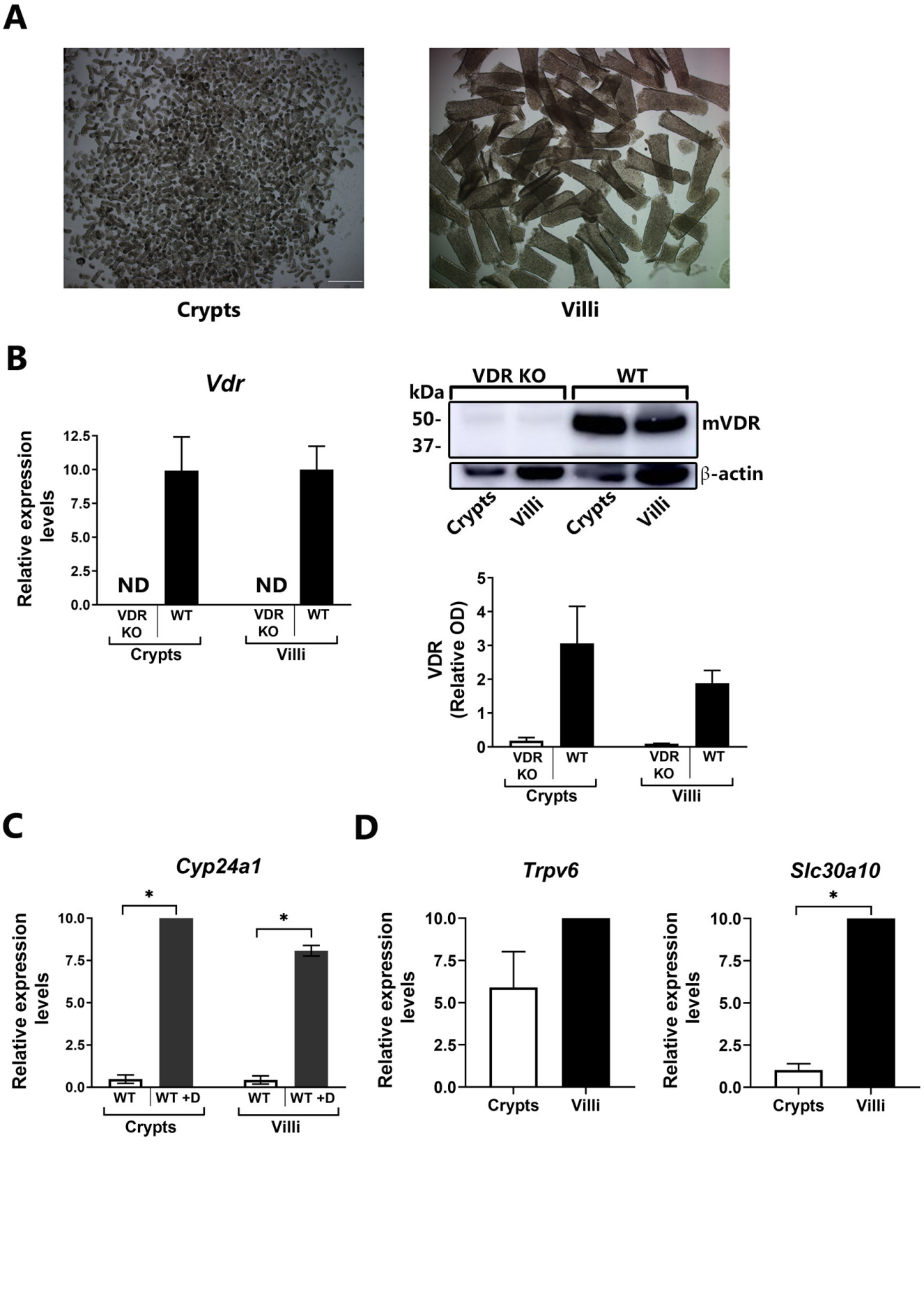

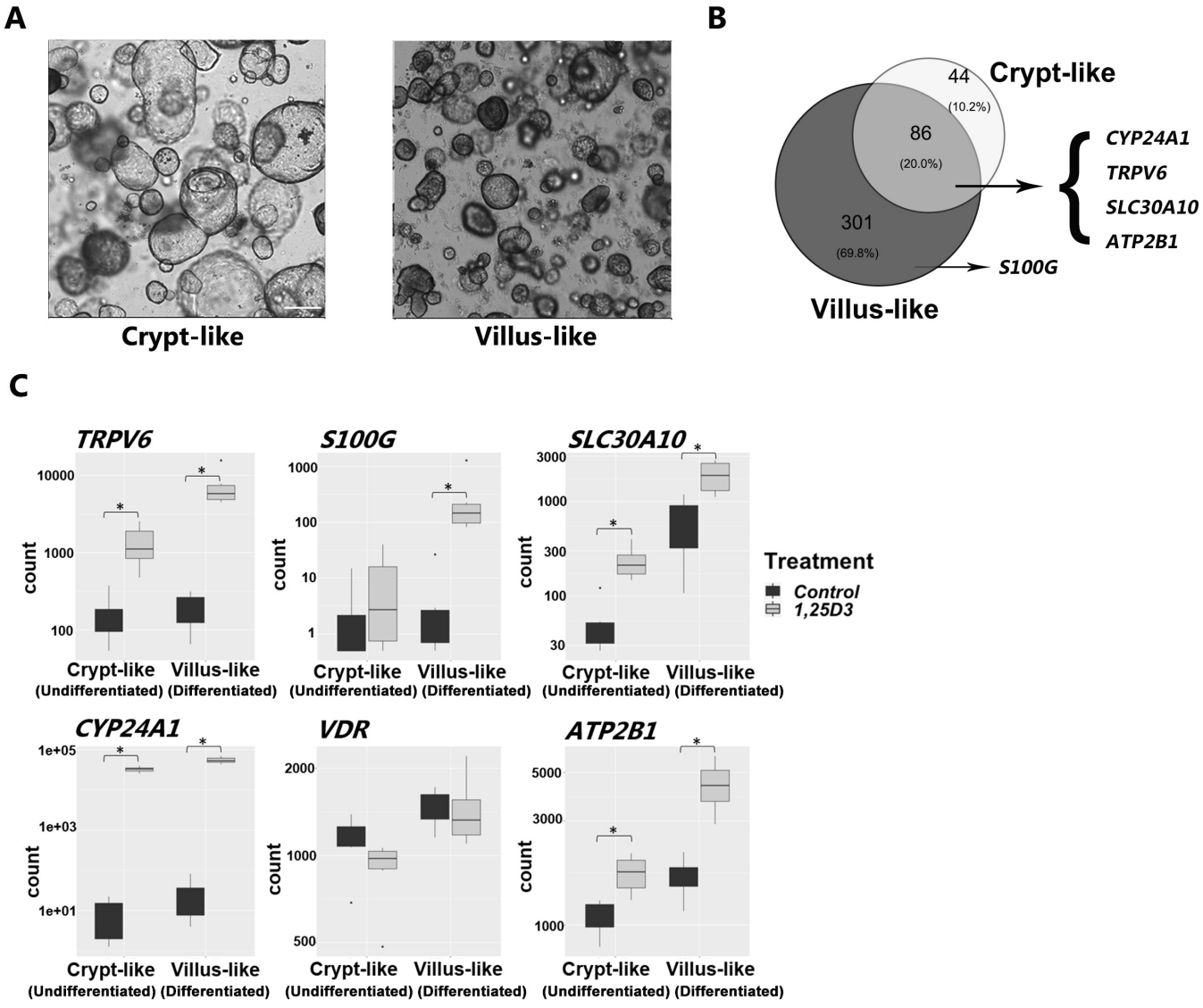

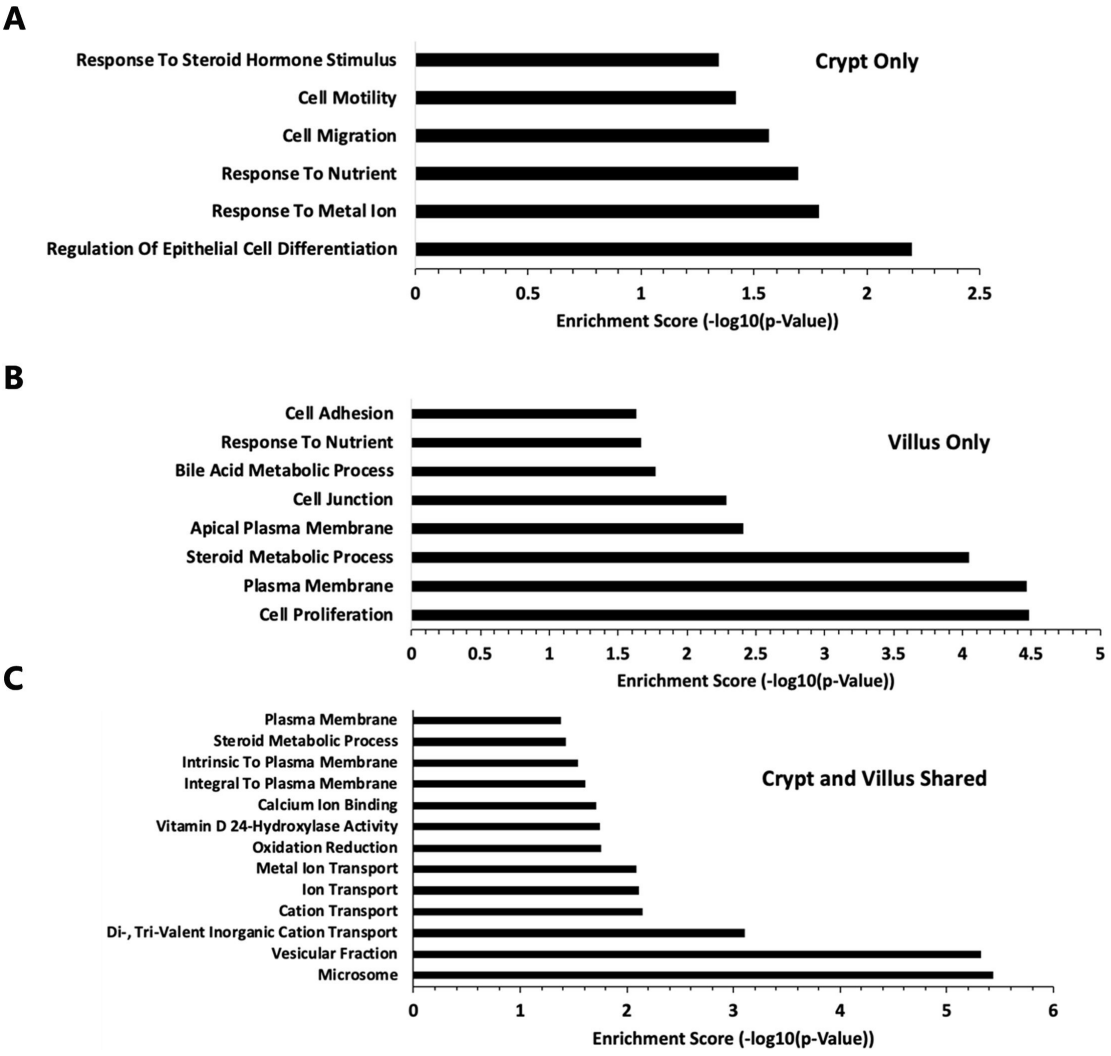

Table 1. Trabecular and Cortical Bone Parameters of control and Slc30a10 KO Mice

	Male		Female	
	Control	**Slc30a10 KO**	**Control**	**Slc30a10 KO**
Trabecular bone				
N	8	5	10	9
BV/TV (%)	6.55 ± 1.60	4.44 ± 1.29	5.41 ± 2.33	4.72 ±1.20
Trabecular number (1/mm)	2.07 ± 0.39	1.48 ± 0.36*	1.62 ±0.57	1.54 ± 0.35
Trabecular thickness (mm)	0.031 ± 0.002	0.030 ± 0.002	0.033 ± 0.002	0.031 ± 0.001*
Cortical bone				
N	8	4	10	8
Cross-sectional tissue area (mm^2)	2.11 ± 0.30	1.35 ± 0.39*	1.92 ± 0.27	1.33 ± 0.16*
Medullary area (mm^2)	1.44 ± 0.23	1.00 ± 0.34*	1.29 ± 0.23	1.03 ± 0.13*
Cortical thickness (mm)	0.124 ± 0.012	0.092 ± 0.023*	0.140 ± 0.011	0.086 ± 0.010*
Porosity (%)	12.07 ± 2.68	6.12 ± 1.12*	9.22 ± 2.07	6.24 ± 1.55*

NOTE. Trabecular bone parameters and cortical bone parameters as measured by µCT.
Data are presented as mean ± SEM (unpaired, two-tailed t test KO vs WT for each sex).
BV/TV, bone volume/tissue volume. *$p < 0.05$.

Table 2 Gene expression of transporters in crypt-like and villus-like human enteroids derived from duodenum treated with $1,25(OH)_2D_3$ or vehicle

Gene	Crypt-like		Villus-like		
	Fold Change	*p* Value	Fold Change	*p* Value	
SLC30A10	5.38	2.05E-19*	3.20	2.99E-03*	Mn efflux transporter
SLC30A4	0.82	5.51E-01	0.93	8.44E-01	Zn transporter
SLC30A5	1.02	9.56E-01	1.05	7.89E-01	Zn transporter
SLC34A2	6.94	5.17E-22*	3.02	3.00E-03*	Phosphate transporter
SLC37A2	1.06	9.63E-01	13.13	8.34E-49*	G6P transporter
TRPM7	0.94	9.22E-01	0.78	1.23E-01	non Slc transporter of divalent cations

*$p < 0.05$.